Two-particle lepton–nucleon interactions at intermediate energies

A. A. Bel'kov

Institute of High Energy Physics, Serpukhov

S. G. Kovalenko

Joint Institute for Nuclear Research, Dubna

Fiz. Elem. Chastits At. Yadra **18**, 110–153 (January–February 1987)

The present state of theory and phenomenology of two-particle lepton–nucleon interactions at intermediate energies is reviewed. The main tendencies in the development of theoretical ideas about the dynamics in these interactions on the basis of QCD are outlined. The dual QCD approach developed by the authors is discussed in detail. The weak and electromagnetic form factors of the nucleon and electroproduction and neutrino-induced production of the Δ_{33} isobar are considered in the framework of this approach. The results of calculations agree well with the available experimental data. The possibility of improving the existing estimates of the QCD parameter Λ by a combined analysis of data on deep inelastic and two-particle lepton–nucleon processes is considered.

INTRODUCTION

The problem of describing two-particle lepton–nucleon processes lies at the transition from low- to high-energy physics, and these are two branches of elementary-particle physics that operate with very different concepts and methods. A fruitful tendency for mutual interpenetration has recently been noted. This leads to a deeper understanding of hadron physics and to the development of new ideas about two-particle lepton–nucleon processes as a source of very important information about the coherent properties of the structure of the nucleon, which appears in the given case as a single entity. In this they differ fundamentally from deep inelastic processes, which probe the "hyperfine" nucleon structure manifested in the region of large momentum transfers (Q^2) and large invariant masses of the final reaction products.

It is well known that the standard formalism of asymptotically free QCD perturbation theory, so effective for studying deep inelastic scattering, has not led to the desired results when applied to exclusive-type processes. Therefore, in contrast to deep inelastic processes, the theoretical interpretation of elastic, quasielastic, and resonance reactions in the framework of QCD has encountered serious difficulties. Reliable results have been obtained in the theory of exclusive processes only in the region of large momentum transfers, $Q^2 \to \infty$. The development of factorization ideas made it possible to recover in QCD the classical quark counting rules[1-2] up to logarithmic factors and make asymptotic calculations to a high level of rigor.[3-6]

However, it was soon found that these ideas are not applicable for the description of real experimental data on form factors. Direct extrapolation of the asymptotic expressions to the region of moderate Q^2 values leads to clear disagreement with the experiments. At the same time, there are also purely theoretical arguments against the validity of such an extrapolation. Indeed, the asymptotic analysis of the form factors[3-6] in the region $Q^2 \to \infty$ establishes dominance of the mechanism of hard quark rescattering.[2] At the same time, direct application of this formalism in the region $Q^2 \sim 10$ GeV^2 shows that the mean momentum transfers between the quarks, i.e., the virtuality of the intermediate gluons, is much less than 1 GeV.[7] This contradicts the very essence of the hard-rescattering mechanism and makes it impossible to use perturbation theory based on asymptotically free QCD. At such virtualities, nonperturbative effects must play the dominant role. The form factors enter the asymptotic region only just below "astronomical" values of the transverse Q^2.[8]

Allowance for nonperturbative effects in the framework of quantum field theory is an extremely difficult problem and has still not yet been definitively solved. Among theoreticians, this circumstance has created a deep pessimism with regard to the possibility of applying QCD to the description of the form factors, while among the experimentalists the so-called dipole parametrization has become more and more popular. This parametrization has been widely used to analyze data on elastic, quasielastic, and resonance interactions and is still used. The results of this analysis are presented in the form of the values deduced from the experiments for the vector and axial masses (M_V, M_A), which occur in the dipole formulas as free parameters. However, one cannot ascribe any definite physical meaning to these quantities, and their extraction does not yield real information about nucleon structure. This is due to the fact that the dipole formulas themselves are purely empirical parametrizations, lacking a theoretical foundation.

Thus, a particularly topical problem is the development of new nonperturbative approaches to the description of exclusive processes at moderate Q^2 in the framework of QCD. Significant process in this direction can be achieved by the combined use of the formalism of asymptotically free perturbation theory and various finite-energy sum rules and dispersion relations. In this case, the nonperturbative effects are concentrated in the phenomenological parameters, which are not calculated but do have a well-defined physical meaning. Such an approach, which has received the general designation of the QCD sum-rule method, was first proposed in Ref. 9 and was applied to the description of the masses and leptonic decay widths of hadrons. The phenomenological nonperturbative parameters are here the vacuum condensates of the quarks, $\langle\bar{q}q\rangle$, and gluons, $\langle G^2\rangle$, which are universal for all processes. An extensive literature has been devoted to the development of this approach,[10-13] which was subsequently generalized to the case of the hadron form factors.[14,15] A good description of the experimental data was achieved in this way.

A different approach to the problem of the nucleon form factors, the dual QCD approach, was developed by the authors of the present review in Refs. 16–19. Like the other, it is based on the use of finite-energy sum rules in perturbative QCD. The two approaches have many common features. In the latter, the entities analyzed are the nucleon structure functions, and this makes it possible to exploit the fruitful ideas of quark–parton phenomenology. The finite-energy sum rules that provide the basis of the dual QCD approach make it possible to relate the physical structure functions of lepton–nucleon processes, containing contributions of resonances and the nucleon peak, to a smooth theoretical function calculated by the methods of QCD perturbation theory. The finite-energy sum rules are obtained on the basis of Wilson operator expansions on the light cone. However, the derivation of these sum rules is not rigorous, since at the present time the structure of the contributions of the Wilson operators of higher twists has not been fully investigated. Therefore, this approach has a semiphenomenological nature, and an important criterion for its consistency is comparison with experimental data. The dual QCD approach gives a realization of Feynman's well-known mechanism in QCD, and this is an alternative to the hard quark rescattering mechanism. In the framework of the approach there is a partonlike picture of the two-particle processes, and the nucleon form factors are expressed in a Lorentz-invariant manner in terms of the quark distribution functions. Its advantages include the fact that it can be applied to any two-particle lepton–nucleon process and also that the calculations are simple. It is also very important that it enables one to relate the physical characteristics of two-particle and deep inelastic lepton–nucleon processes and analyze them together. This increases the reliability of the information extracted from the experimental data about the quark distributions in the nucleon and the value of the fundamental QCD parameter Λ. The inclusion of data on the two-particle reactions makes it possible to eliminate in the determination of these quantities numerous uncertainties that arise from an independent analysis of deep inelastic scattering and are associated with the region of large values of the Bjorken variable x. In the combined analysis, the two-particle processes become a source of additional information about the behavior of the structure functions in this region.

We begin the consideration of two-particle lepton–nucleon processes with a discussion of some general questions of their phenomenology and the experimental status of the problem.

1. ELASTIC AND QUASIELASTIC LEPTON–NUCLEON SCATTERING

Processes of elastic and quasielastic lepton–nucleon scattering are described by means of form factors that determine the structure of the matrix elements of the electromagnetic and weak hadronic currents:

$$\left.\begin{aligned} &\langle N'(p')\mid J_\mu^{em}\mid N(p)\rangle = \\ &=\bar{u}(p')\left[F_1(Q^2)\gamma_\mu+\frac{\sigma_{\mu\nu}q_\nu}{2M_N}F_2(Q^2)\right]u(p); \\ &\langle N'(p')\mid J_\mu^{w}\mid N(p)\rangle=\bar{u}(p')\left[\gamma_\mu F_V(Q^2)+\right. \\ &\left.+\frac{\sigma_{\mu\nu}q_\nu}{2M_N}F_M(Q^2)+\gamma_\mu\gamma_5F_A(Q^2)+\frac{q_\mu\gamma_5}{M_N}F_P(Q^2)\right]u(p). \end{aligned}\right\} \quad (1)$$

Here, J_μ^{em} is the electromagnetic current, J_μ^{w} is the charged or neutral weak current, $q=p'-p$, $Q^2=-q^2$, and $F_{1,2}$ and $F_{V,M,A,P}$ are, respectively, the electromagnetic and weak form factors, assumed real by virtue of T invariance.

From conservation of the vector current (CVC) there follows a connection between the weak form factors F_{VM}^{CC} for the charged current and the electromagnetic form factors $G_{E,M}$:

$$F_{V,M}^{CC}=F_{1,2}^{p}-F_{1,2}^{n}, \quad (2)$$
$$F_1=(G_M-G_E)/\tau,\quad F_2=\left(G_E+\frac{Q^2}{4M_N^2}G_M\right)\Big/\tau,$$

where $\tau=1+Q^2/(4M_N^2)$; $F_1^{p,n}(Q^2)$ and $F_2^{p,n}(Q^2)$ are the Dirac and Pauli form factors of the proton and neutron. From the structure of the weak neutral current in the Weinberg–Salam model,

$$J_\mu^{NC}=J_\mu^{(3)}-2\sin^2\theta_W J_\mu^{em} \quad (3)$$

($J^{(3)}$ is the isovector current), and CVC we obtain a connection between the form factors $F_{V,M,A}^{NC}$ for the neutral current and the form factors $F_{V,M,A}^{CC}$ and the electromagnetic form factors

$$F_{V,M}^{NC}=\frac{1}{2}F_{V,M}^{CC}-2\sin^2\theta_W F_{1,2};\quad F_A^{NC}=\frac{1}{2}F_A^{CC}. \quad (4)$$

For the electromagnetic form factors there are also scaling relations,

$$G_E^p=G_M^p/\mu_p=G_M^n/\mu_n,\quad G_E^n=0, \quad (5)$$

where $\mu_p=2.79$ and $\mu_n=-1.91$ are the proton and neutron magnetic moments, and $G_E^p(0)=1$.

The hypothesis of partial conservation of the axial-vector current (PCAC) relates the divergence of the strangeness-conserving axial hadronic current to the pion field φ_π:

$$\partial_\mu A_\mu=m_\pi^2 f_\pi\varphi_\pi, \quad (6)$$

where $f_\pi=94$ MeV is the $\pi\to\mu\nu$ decay constant. In accordance with PCAC, the contribution of the axial-vector current to the weak processes at small Q^2 is largely determined by the pion pole, and

$$F_p(Q^2)\approx 2M_N^2F_A(Q^2)/(Q^2+m_\pi^2), \quad (7)$$

$$F_A(0)=-g_A=-\frac{f_\pi g_{\pi N}}{M_N}\ \text{(Goldberger–Treiman relation)},$$

where $g_{\pi N}$ is the constant of the πN interaction, and $g_A=1.23$ is the axial coupling constant, measured in neutron β-decay experiments. The contribution of the pseudoscalar form factor F_p to the cross section of quasielastic (elastic) scattering of neutrinos is proportional to the mass of the lepton in the final state, and therefore the term with F_p in (1) can be ignored.

The experimental nucleon form factors are determined in experiments on elastic eN scattering, the differential cross section of which in the approximation of one-photon exchange is described by Rosenbluth's formula[20]

$$\frac{d\sigma}{d\Omega_e}=\frac{\alpha^2}{4E^2}\,\frac{\cos^2(\theta/2)}{\sin^4(\theta/2)}\,\frac{1}{2M\eta}\,[1+\delta'(Q^2)]$$

$$\times\left[\frac{2M_N G_E^2(Q^2)+\dfrac{Q^2}{2M_N}\,G_M^2(Q^2)}{1+Q^2/(4M_N^2)}+2\tan\left(\frac{\theta}{2}\right)\frac{Q^2}{2M_N}\,G_M^2(Q^2)\right]. \quad (8)$$

Here, α is the fine-structure constant, θ is the scattering angle in the laboratory system, E is the energy of the incident electron, $\eta=1+(2E/M_N)\sin^2(\theta/2)$, and $\delta'(Q^2)$ is a correction that arises when allowance is made for higher orders in α in the electron–photon vertex[21]:

$$\delta'(Q^2)=\frac{2\alpha}{\pi}\left(\frac{13}{12}\log\frac{Q^2}{m_e^2}-\frac{14}{9}\right).$$

The experimental data[22-27] show that the scaling relations (5) are satisfied to within 5%. The most accurate measurements have been made of the proton electromagnetic form factors, whose dependence on Q^2 is usually approximated by the dipole formula

$$G_E^p(Q^2)=G_M^p(Q^2)/\mu_p=G_{\mathrm{DIP}}(Q^2)=(1+Q^2/M_V^2)^{-2}, \quad (9)$$

where M_V is the vector mass. The best agreement with experiment is obtained for $M_V=0.84$ GeV. However, the dipole parametrization (9) does not have a reliable theoretical justification. Moreover, there are appreciable deviations of the experimental data[28] from the simple dipole dependence (9):

$$G_E^p(Q^2)=G_M^p(Q^2)/\mu_p=\lambda(Q^2)\,G_{\mathrm{DIP}}(Q^2). \quad (10)$$

The correcting factor $\lambda(Q^2)$ is shown in Fig. 1.

The nucleon weak form factors are extracted from analysis of the differential cross sections $d\sigma/dQ^2$ of quasielastic (elastic) νN scattering:

$$\frac{d\sigma^{\pm}}{dQ^2}=\frac{G^2}{\pi}\left\{\left(\frac{F_V\pm F_A}{2}\right)^2+(1-y)^2\left(\frac{F_V\mp F_A}{2}\right)^2-\frac{1}{2}(F_V^2-F_A^2)\frac{Q^2}{2E_\nu^2}+\frac{F_M}{2}y\left[F_M(1-y)\frac{E_\nu}{2M_N}+\frac{y}{4}(4F_V+F_M\mp 4F_A)\pm F_A\right]\right\}, \quad (11)$$

where the coupling constant is $G^2=5\cdot10^{-38}\ \mathrm{cm}^2\cdot\mathrm{GeV}^{-2}$, $y=Q^2/(2M_N E_\nu)$, E_ν is the neutrino (antineutrino) energy, and the upper and lower signs correspond to neutrino and antineutrino scattering, respectively.

The validity of CVC is usually assumed, and one uses the connection between the weak form factors $F_{V,M}$ and the electromagnetic form factors $G_{E,M}$, which are parametrized by the dipole formula $G_E(Q^2)=G_M(Q^2)/(\mu_p)=\lambda(Q^2)(1+Q^2/M_V^2)^{-2}$. The experimental data on the differential cross section (11) are then used to extract information about the axial form factor F_A. In the majority of cases,[29-32] one again uses the dipole parametrization of the axial form factor,

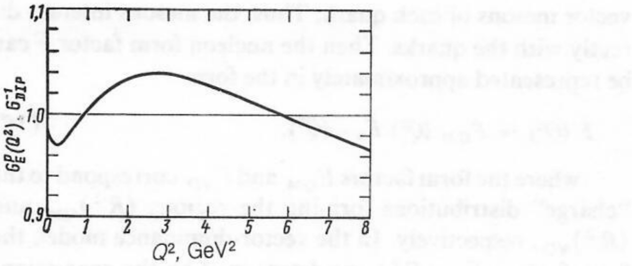

FIG. 1. Deviation of the experimentally measured electromagnetic form factor $G_E^p(Q^2)$ of the proton from the dipole parametrization $G_{\mathrm{DIP}}=(1+Q^2/0.71)^{-2}$.

$$F_A(Q^2)=F_A(0)/(1+Q^2/M_A^2)^2,\quad F_A(0)=-1.23, \quad (12)$$

and the experimentally measured parameter is assumed to be the axial mass M_A. The best agreement with experiment is obtained for the value $M_A\approx1$ GeV. Quasielastic neutrino and antineutrino scattering has been the most fully studied.[29-32] Data on νN scattering are as yet sparse and insufficiently reliable.[33-35]

The accuracy of the experimental data on quasielastic νN scattering does not yet permit measurement of the deviation of the Q^2 dependence of the axial form factor F_A from the dipole parametrization (12). Nevertheless, there are already indications of such a deviation.[36] This circumstance, and also the fact that the dipole parametrization of the nucleon electromagnetic and weak form factors does not have a theoretical justification, make it necessary to look for other approaches to the description of the nucleon form factors. We shall consider some of them in the following sections of the present review, devoting the main attention to the dual QCD approach that we have developed and its applications. But here, as an alternative to the dipole parametrization of the nucleon form factors, we consider the parametrization in the framework of the model of vector-meson dominance and its modifications at the quark level.

The hypothesis of vector-meson dominance establishes a connection of the isotriplet of vector ($\mathbf{V}_\mu$) and axial-vector ($\mathbf{A}_\mu$) currents and the fields of the vector and axial-vector mesons:

$$\mathbf{V}_\mu=\frac{m_\rho^2}{g_\rho}\,\boldsymbol{\rho}_\mu,\quad \mathbf{A}_\mu=g_{A_1}\frac{m_\rho^2}{g_\rho^2}\,\mathbf{a}_\mu. \quad (13)$$

Here, $\boldsymbol{\rho}_\mu$ and $\mathbf{a}_\mu$ are the fields of the ρ and A_1 mesons, and g_ρ and g_{A_1} are the corresponding coupling constants. In accordance with (13), the dominance model gives for the nucleon form factors the predictions

$$\left.\begin{aligned}&G_E^p(Q^2)=G_M^p(Q^2)/\mu_p=m_\rho^2/(Q^2+m_\rho^2);\\&F_V^{CC}(Q^2)=m_\rho^2/(Q^2+m_\rho^2);\quad F_A^{CC}(Q^2)=g_A m_{A_1}^2/(Q^2+m_{A_1}^2).\end{aligned}\right\} \quad (14)$$

However, these formulas do not describe the experimental data well. Therefore, attempts have been made to modify the vector-dominance model at the quark level. We discuss two possible modifications.[36,37]

We adopt a geometrical picture, in accordance with which the mean-square nucleon radius $\langle R^2\rangle$ is made up of the radius $\langle R^2\rangle_{\mathrm{QM}}$ of the region of confinement of the quarks, determined by the wave function of their bound state, and the radius $\langle R^2\rangle_{\mathrm{VD}}$ of the cloud of vector and axial-vector mesons of each quark. Thus, the mesons interact directly with the quarks. Then the nucleon form factor F can be represented approximately in the form

$$F(Q^2) = F_{QM}(Q^2)\, F_{VD}(Q^2), \tag{15}$$

where the form factors F_{QM} and F_{VD} correspond to the "charge" distributions forming the regions $\langle R^2\rangle_{QM}$ and $\langle R^2\rangle_{VD}$, respectively. In the vector-dominance model, the form factors $F_{VD}(Q^2)$ are determined by the expressions (14). The form factor F_{QM} is determined by the wave function of the quarks in the nucleon and is introduced in different ways depending on the chosen model.

The simplest empirical parametrization of the form factor F_{QM} that describes the experimentally observed behavior of the nucleon vector form factor has the form[38]

$$F_{QM}(Q^2) = \exp\left[-\frac{1}{6}Q^2R^2/(1+Q^2/(4M_N^2))\right], \tag{16}$$

where $R^2 = 6\,\mathrm{GeV}^{-2}$. In this model, the nucleon vector and axial form factors have the form[36]

$$F_{V,A}(Q^2) = \frac{F_{V,A}(0)\exp\left[-\frac{1}{6}Q^2R^2\Big/\left(1+\frac{Q^2}{4M_N^2}\right)\right]}{1+Q^2/m^2_{\rho,A_1}}, \tag{17}$$

where $F_V(0) = 1$ and $F_A(0) = -1.23$. Direct numerical calculations show that the parametrization (17) for the vector form factor F_V hardly differs from the dipole parametrization, whereas the axial form factor F_A calculated in accordance with (17) in the region $Q^2 \approx 0.5\,\mathrm{GeV}^2$ is 10% greater than the dipole form factor (12). Figure 2 compares the differential cross sections of the $\nu_\mu n \to \mu^- p$ reaction calculated for the dipole parametrization of the nucleon form factors and for the parametrization (17). In the region $Q^2 \approx 0.5$ GeV^2 at $M_A = 1$ GeV the difference between the differential cross sections $d\sigma/dQ^2$ reaches 3%. Analysis of the experimental data[30] showed that fitting of the differential cross section of quasielastic νN scattering to the parametrization (17) of the nucleon form factors is better by one standard deviation than to the dipole formula.

A different representation of the form factor F_{QM} in Eq. (15) was considered in Ref. 37 on the basis of the dynamical model of factorized quarks.[39] According to this model, the incident particle ($W^\pm$, Z^0, γ^*) excites in the nucleon an effective potential $V_{\mathrm{eff}}(r)$, on which quasielastic scattering of the constituent quarks occurs. The potential $V_{\mathrm{eff}}(r)$ is given in the relativistic configuration representation[40] and

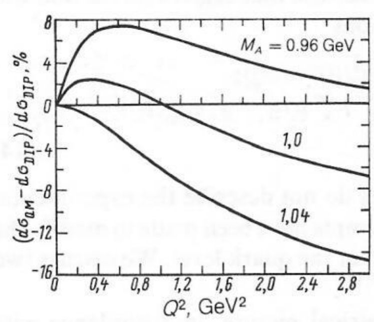

FIG. 2. Difference between the differential cross sections of $\nu_\mu n \to \mu^- p$ quasielastic scattering for different parametrizations of the nucleon form factors: σ_{DIP} is the cross section calculated with the dipole parametrization, and σ_{QM} is the cross section calculated with the parametrization (17) in the modified vector-dominance model.

has the form $V_{\mathrm{eff}}(r) = \delta(r)/(4\pi r^2)$. Then for the quark scattering amplitude g_i we obtain

$$g_i(Q_i^2) = y_i/\mathrm{sh}\, y_i,\quad y_i = \mathrm{Arch}\,(1 - Q_i^2/2m_i^2), \tag{18}$$

where Q_i^2 is the 4-momentum transfer on one quark of mass m_i (for simplicity, one can assume $m_i = m_N/3$, $\sqrt{Q_i^2} = \sqrt{Q^2}/3$). In the considered case, the nucleon form factor is proportional to the product of the amplitudes of quark scattering by the potential V_{eff} and

$$F_{QM}(Q^2) \sim g_i^3(Q^3). \tag{19}$$

Thus, in this model the nucleon vector and axial form factors have the form

$$F_{V,A}(Q^2) = F_{V,A}(0)\,\frac{g_i^3(Q^2)}{1+Q^2/m^2_{\rho,A_1}}. \tag{20}$$

Since $g_i(0) = 1$, the factor $g_i^3(Q^2)$ in (20) does not distort the normalization of the nucleon form factors at $Q^2 = 0$. The use of the expression (20) leads to a better description of the experimental data than do the dipole formula and the parametrization (17).

2. ELECTROPRODUCTION AND NEUTRINO-INDUCED PRODUCTION OF THE ISOBAR Δ_{33}

The processes of electroproduction ($ep \to \Delta^+ e$) and neutrino-induced production ($\nu_\mu\, p \to \mu^- \Delta^{++}$) of the Δ_{33} isobar are described by means of six form factors, which occur in the matrix elements of the electromagnetic and weak hadronic currents:

$$\left.\begin{aligned}
&\langle \Delta_{33}(p') \mid J_\mu^{em} \mid N(p)\rangle = \bar\psi_\nu(p')\left[\frac{C_3}{M_N}(\hat q g_{\mu\nu} - q_\nu\gamma_\mu)\right.\\
&\left.+\frac{C_4}{M_N^2}((p'q)\, g_{\mu\nu} - q_\nu p'_\mu)\right]\gamma_5 u(p);\\
&\langle \Delta_{33}(p') \mid J_\mu^{w} \mid N(p)\rangle = \bar\psi_\nu(p')\left\{\left[\frac{C_3'}{M_N}(\hat q g_{\mu\nu} - q_\nu\gamma_\mu)\right.\right.\\
&\left.+\frac{C_4^V}{M_N^2}((p'q)\, g_{\mu\nu} - q p'_\mu)\right]\gamma_5 + \frac{C_3^A}{M_N}(\hat q g_{\mu\nu} - q_\nu\gamma_\mu)\\
&\left.+\frac{C_4^A}{M_N^2}((p'q)\, g_{\mu\nu} - q_\nu p'_\mu) + C_5^A g_{\mu\nu} + \frac{C_6^A}{M_N^2} q_\nu q_\mu\right\} u(p).
\end{aligned}\right\} \tag{21}$$

Here, $\bar\psi_\nu$ is a Rarita–Schwinger spinor describing states with spin 3/2, $q = p' - p$, $C_{3,4}$ are the electroproduction form factors of the Δ^+ isobar, and $C^V_{3,4}$, C_i^A ($i = 3,\ldots, 6$) are the form factors for neutrino-induced production of the Δ^{++} isobar corresponding to interaction with the weak vector and axial currents. By T invariance, all form factors are assumed to be real functions of $Q^2 = -q^2$.

From CVC and the assumption of dominance of the magnetic dipole transition (M_1)[41-44] there follows a connection between the electromagnetic form factors C_3 and C_4:

$$C_4 = -\frac{M_N}{W} C_3, \tag{22}$$

where W is the effective mass of the πN system into which the Δ isobar decays. Since $\langle \Delta^{++} | V_\mu | p\rangle = \sqrt{3}\,\langle \Delta^+ | J_\mu^{\mathrm{em}} | p\rangle$, where V_μ is the strangeness-conserving weak hadronic current, the form factors $C^V_{3,4}$ for neutrino-induced production of the isobar are related to the electromagnetic form factors by

$$C^V_{3,4} = \sqrt{3}\, C_{3,4}. \tag{23}$$

From PCAC we obtain for the axial form factors of Δ^{++} isobar neutrino-induced production the relations

$$\left.\begin{aligned} C_6^A(Q^2) &= M_N^2 C_5^A(Q^2)/(Q^2+m_\pi^2); \\ C_5^A(0) &= \sqrt{\frac{2}{3}}\,\frac{f_\pi g_{\Delta N\pi}}{m_\pi} = 1{,}2, \end{aligned}\right\} \qquad (24)$$

where $g_{\Delta N\pi} = 2.11$ is the $\Delta^{++} \to p\pi^+$ decay constant.

The electroproduction of the Δ^+ isobar has by now been well studied. Its differential cross section can be expressed as follows in terms of the helicity amplitudes $f_{\pm,0}$ and the scattering angle θ of the electron in the laboratory coordinate system[45]:

$$\frac{d\sigma}{d\Omega_e} = \frac{\alpha^2\cos^2(\theta/2)}{4E^2\sin^4\left(\frac{\theta}{2}\right)\left[1+2\frac{E}{M_N}\sin^2\left(\frac{\theta}{2}\right)\right]} \times \left[\left(\frac{Q^2}{\widetilde{Q}^2}\right)^2|f_0|^2 + \left(\frac{|Q^2|}{2\widetilde{Q}^2} + \frac{M_\Delta^2}{M_N^2}\tan^2\left(\frac{\theta}{2}\right)\right)(|f_+|^2+|f_-|^2)\right], \qquad (25)$$

where E is the energy of the final electron, and $\widetilde{Q}^2 = |Q^2| + (1/4M_\Delta^2)(M_\Delta^2 - M_N^2 - |Q^2|)^2$ is the square of the 3-momentum transferred to the nucleon in the Δ_{33} rest frame.

For analysis of the experimental data on Δ_{33} electroproduction one usually employs instead of the helicity amplitudes the $N\Delta$ transition form factors $G_{M\Delta}$, $G_{E\Delta}$, and $G_{C\Delta}$:

$$G_{M\Delta}^2(Q^2) + G_{E\Delta}^2(Q^2) = \frac{2M_N^2}{\widetilde{Q}^2}(|f_+|^2+|f_-|^2),$$

$$G_{C\Delta}^2(Q^2) = \frac{2M_N^2}{\widetilde{Q}^2}|f_0|^2. \qquad (26)$$

The form factors $G_{M\Delta}$, $G_{E\Delta}$, and $G_{C\Delta}$ correspond to excitations of the type M_1, E_2, and C_2 (Coulomb octupole), giving rise to the transition $J = 1/2^+ \to J = 3/2^+$. There are theoretical[41,42] and experimental[43,44] indications that the form factors $G_{E\Delta}$ and $G_{C\Delta}$ must be much less than $G_{M\Delta}$ (dominance of the dipole magnetic transition M_1). Therefore, in the analysis of the angular distributions (25) of the electron the form factors $G_{E\Delta}$ and $G_{C\Delta}$ are usually ignored and only $G_{M\Delta}$ is directly extracted, being measured with high accuracy in a wide range of Q^2 values.[46] Analysis of data on the $ep \to e\Delta^+$ reaction in the language of the form factors $C_{3,4}$ (21) showed that the best description of experiment is obtained using the parametrization[47]

$$|C_3(Q^2)|^2 = (2.05)^2\,[1 + 9\sqrt{Q^2}]\,\exp\left[-6{,}3\sqrt{Q^2}\right]. \qquad (27)$$

The $\nu_\mu p \to \mu^- \Delta^{++}$ process, which makes the main contribution to the production of single charged pions in νp interactions, has also been well studied.[48-51] For this process, the total cross sections have been measured in a wide range of neutrino energies E_ν, as have the differential cross sections $d\sigma/dQ^2$. The latter are of great interest not only for extracting information about the form factors of neutrino-induced production of the Δ^{++} isobar but also for verification of PCAC, in accordance with which

$$\frac{d\sigma}{dQ^2}(Q^2=0) = \frac{G^2}{4\pi}\,\frac{s-W^2}{s-M_N^2}\,\frac{M_N+W}{M_N}\,(C_5^A(0))^2, \qquad (28)$$

where s is the square of the total effective mass. Extrapolation of the experimental data to the point $Q^2 = 0$ showed that the PCAC relation holds to within the experimental errors of $\pm 20\%$.[48]

In the analysis of experimental data on the $\nu_\mu p \to \mu^- \Delta^{++}$ reaction the vector form factors $C_{3,4}^V$ are fixed by means of the relations (23) and (27), and information about the axial form factors $C_{3,4,5}^A$ is extracted. These form factors are parametrized as follows:

$$C_i^A(Q^2) = C_i^A(0)\left(1 + \frac{a_i Q^2}{b_i + Q^2}\right)\Big/(1 + Q^2/M_A^2)^2, \qquad (29)$$

where $C_3^A(0) = 0$, $C_4^A(0) = -0.3$, $C_5^A(0) = 1.2$, $a_{4,5} = -1.21$, $b_{4,5} = 2.0$ in Adler's model[52]; $C_3^A(0) = 1.8$, $a_3 = -1.11$, $b_3 = 0.63$, $C_4^A(0) = -1.8$, $a_4 = -1.05$, $b_4 = 0.77$, $C_5^A(0) = 1.9$, $a_5 = -1.11$, $b_5 = 1.32$ in Zucker's model[53]; M_A is the axial mass, a free parameter that is determined from experiment. Analysis of the data[48] showed that the best agreement with experiment is given by the parametrization (29) in Adler's model, and Zucker's model can be rejected on the basis of the χ^2 test. For the axial mass, the result $M_A \approx 1$ GeV is obtained in all cases. The achieved accuracies do not yet permit one to speak of any significant deviations of the results of experiment from calculations with the dipole parametrization (29). However, the lack of a theoretical justification of this parametrization casts doubt on the physical significance of the data analysis based on it.

3. NUCLEON FORM FACTORS IN QCD

The description of the hadron form factors in the framework of quantum field theory is a difficult but urgent problem of elementary-particle physics. The general features of the asymptotic behavior of the form factors were established in the classical study of Ref. 1 by dimensional analysis. As a result, quark counting rules were formulated, and these became an inseparable part of modern ideas about the form factors of composite particles. The quark counting rules prescribe the following asymptotic behavior for the form factor of a hadron consisting of n quarks:

$$F(Q^2) \underset{Q^2\to\infty}{\longrightarrow} \frac{1}{(Q^2)^{n-1}}. \qquad (30)$$

In Ref. 2, a dynamical mechanism realizing such behavior of the form factors was found—the mechanism of hard quark rescattering, shown graphically in Fig. 3. It was justified in QCD on the basis of perturbation theory. It was established[3-6] that in QCD the power law (30) is satisfied up to a logarithmic factor. In particular, the nucleon magnetic form factor G_M has the asymptotic behavior

$$G_M(Q^2) \underset{Q^2\to\infty}{\longrightarrow} \left(\frac{\alpha_s(Q^2)}{Q^2}\right)^2 (\alpha_s(Q^2))^{C_F/\beta_0}. \qquad (31)$$

Here, $\alpha_S = 4\pi/(\beta_0 \ln(Q^2/\Lambda^2))$ is the chromodynamical running coupling constant in the leading order, $\beta_0 = 11 - (2/3)n_f$, $C_F = 4/3$, and n_f is the number of flavors.

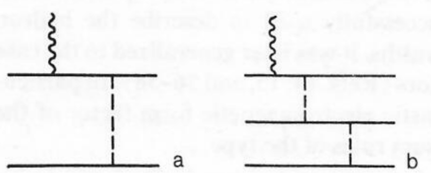

FIG. 3. Diagrams responsible for the asymptotic behavior of the form factors of the pion (a) and nucleon (b).

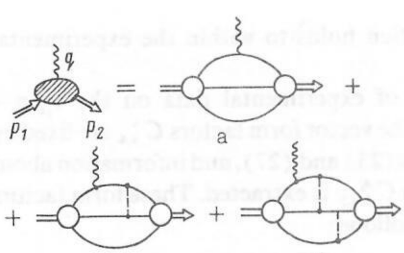

FIG. 4. Structure of the factorization for the nucleon form factors. The generalized quark–hadron vertices together with the quark lines directly next to them correspond to large distances (small virtualities), while the remaining quark and gluon lines correspond to short distances, i.e., virtualities greater than a certain hadronic scale $\lambda^2 \sim 1\ \text{GeV}^2$.

However, the expressions (30) and (31) do not solve the problem of describing the experimental data, since they are essentially asymptotic. Hopes that the form factors enter the asymptotic region at comparatively small Q^2 were not justified. We can give here the following theoretical argument. Following the standard procedure for separating the contributions of large and small distances, we represent the nucleon form factor in the form of the sum of diagrams in Fig. 4. Essentially, such a representation amounts to successive separation from the quark–hadron vertex of various configurations of "hard" quark and gluon lines, through which a large momentum flows. As can be seen from Fig. 4, the hard-rescattering diagram is only the third term of this expansion. It is easy to estimate the relative contribution of each of the three diagrams in Fig. 4. At $Q^2 = 0$, the main contribution is made by the diagram of Fig. 4(a), since in this case there is no large Q^2 and the quark-hadron vertices do not contain a hard component. The following diagrams presuppose the presence of a large momentum. Their contribution is suppressed compared with the first diagram by factors of order $\alpha_S(M_N)\pi \lesssim 0.1$ and $[\alpha_S(M_N)/\pi])^2 \leqslant 0.01$, respectively. Thus, the following picture emerges. In a certain region of momentum transfers $Q^2 < t_{\max}$ the simplest diagram [Fig. 4(a)] is dominant. With increasing Q^2 the mechanism of suppression of this diagram due to the presence of the rapidly decreasing Sudakov form factor of the active quark comes into play. As a result, only the hard rescattering diagram of Fig. 4(c) survives in asymptotia, as was to be expected. According to rough estimates, $t_{\max} \sim (\alpha_S/\pi)^{-2} \cdot 1\ \text{GeV}^2$. Thus, the asymptotic perturbative methods developed in QCD and used successfully to analyze deep elastic scattering do not solve the problem of the nucleon form factors in the region of realistic Q^2 values, since the dominant diagram of Fig. 4(a) corresponds to the nonperturbative contribution. The need for nonperturbative QCD methods arises.

Significant progress in this question is associated with the use of dispersion sum rules and the idea of quark–hadron duality. Such an approach, which has acquired the general name of the method of QCD sum rules, was proposed in Ref. 9 and has been successfully used to describe the hadron masses and decay widths. It was later generalized to the case of hadron form factors (Refs. 14, 15, and 56–58). In particular, study of the elastic electromagnetic form factor of the nucleon[56] yielded sum rules of the type

$$\int_0^{S_0} ds_1 \int_0^{S_0} ds_2\, \rho_i^{Pt}(s_1, s_2, t) = \int_0^{S_0} ds_1 \int_0^{S_0} ds_2\, \rho_i^{\text{Ph}}(s_1, s_2, t) = \pi^2 \lambda_N^2 F_i(t), \quad (32)$$

which are well justified in the framework of realistic assumptions about the nucleon wave function. Here, $\rho_i^{\text{Ph}}(s_1, s_2, t)$ are the physical (containing nonperturbative contributions) and $\rho_i^{\text{Pt}}(s_1, s_2, t)$ are the perturbative (calculated by perturbation theory) spectral densities, S_0 is the duality interval, and λ_N is a normalization constant.

The last equation in (32), which establishes the connection between ρ^{Pt} and the nucleon form factors F_i, follows from the usual approximation of the physical spectral density:

$$\rho_i^{\text{Ph}}(s_1, s_2, t) = \pi^2 \lambda_N^2 F_i(t)\, \delta(s_1 - M_N^2)\, \delta(s_2 - M_N^2). \quad (33)$$

This approach gives good results in the description of experimental data[59] on the elastic nucleon electromagnetic form factors (Fig. 5).

The authors of the present review developed independently a different approach to the problem of the nucleon form factors, similar in its logical structure to the one just described but not related directly to the method of QCD sum rules. Its basis is also the use of sum rules and quark–hadron duality in QCD. The basic physical assumptions of our approach are less general and restrict the region of its applicability to scattering problems. But it does have numerous advantages, which, in particular, make it possible to relate two-particle processes to deep inelastic scattering processes. In turn, this makes it possible to use the formalism of QCD perturbation theory and the well-tested ideas of quark–parton phenomenology.

We now turn to a detailed exposition of the dual QCD approach and consider various applications of it.

4. LOCAL DUALITY AND SUM RULES FOR STRUCTURE FUNCTIONS OF LEPTON–NUCLEON SCATTERING

The physical basis of the dual QCD approach is the idea of Bloom and Gilman[60] of local duality, generalized in the framework of QCD and consistent with its predictions. Duality in lepton–nucleon interactions establishes a connection between the Q^2 dependence of the elastic nucleon peak and nucleon resonances and the behavior of the smooth scaling function $F'(x') = \lim_{Q^2 \to \infty} F(x', Q^2)$, where $F(x', Q^2)$ is the lepton–nucleon scattering structure function. Here, instead of the usual Bjorken variable $x = Q^2/(2M_N\nu)$ we have introduced as the scaling variable $x' = x/(1 + x^2 M_N^2/Q^2)$, with respect to which early scaling is observed (ν and $Q^2 = -q^2$ are the energy and the square of the 4-momen-

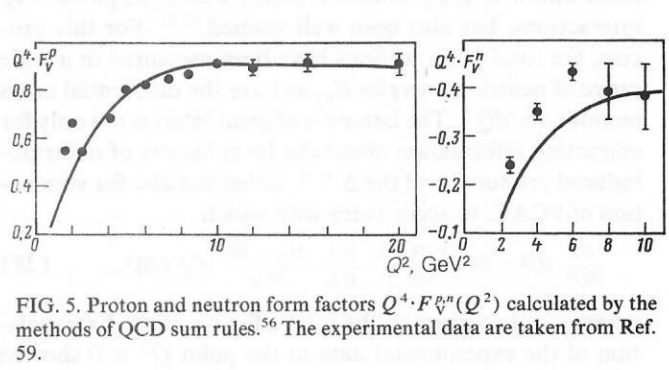

FIG. 5. Proton and neutron form factors $Q^4 \cdot F_V^{p,n}(Q^2)$ calculated by the methods of QCD sum rules.[56] The experimental data are taken from Ref. 59.

tum transferred to the nucleon in its rest frame).

The connection takes the form that the resonances contained in the experimental data at small values of the invariant masses W coincide with the smooth scaling function $F'(x')$ in the sense of the mean value over a sufficiently large kinematic region (global duality). It is obvious that the resonances themselves do not possess scaling, since any dimensionless nucleon–resonance transition form factor $G(Q^2/m^2)$ must contain some dimensional parameter m^2. For purely kinematic reasons, resonances tied to definite values of W are displaced when Q^2 increases to the point $x=1$. This displacement takes place in such a way that duality between the resonances and the smooth function $F'(x')$ must be satisfied. As was shown in Ref. 60, duality must also be valid in a local version, i.e., in the neighborhood of each individual resonance and, more unexpectedly, in the neighborhood of the elastic nucleon peak.

A basis for understanding Bloom–Gilman duality from the point of view of field-theory QCD ideas was found in Refs. 61 and 62 in the form of the relation

$$\int_0^1 d\xi\xi^n \left(F(\xi, Q^2) - F^{(\mathrm{th})}(\xi, Q^2)\right) = \sum_{k=1}^{\infty} B_{n,k}(Q^2)\left(n\frac{M_0^2}{Q^2}\right)^k, \quad (34)$$

which is obtained in the formalism of Wilson operator expansions on the light cone. In this relation, $F(\xi, Q^2)$ is a combination of physical, experimentally observable, structure functions. In the region of resonances, $F(\xi, Q^2)$ contains corresponding resonance peaks and at $W=M_N$ the elastic nucleon peak. The structure function $F^{(\mathrm{th})}(\xi, Q^2)$ is calculated by QCD perturbation theory and has logarithmic behavior with respect to Q^2. This is the smooth function, the analog of the Bloom–Gilman limiting scaling function. It corresponds to the leading contribution in $1/Q^2$ in the expression (34), which is determined by Wilson operators of twist $\tau=2$. The power-law corrections in $(M_0^2/Q^2)^k$ in (34) correspond to the contribution of the operators of higher twists $\tau=2k+2>2$, whose matrix elements are $B_{k,n}(Q^2)M_0^{4k+4}$. The scale M_0 of the power-law corrections is determined by the intrahadron dynamics. The scale could be the mean transverse momentum p_T of the quarks within the nucleon, $M_0 \sim p_T \sim 1/R_{\mathrm{conf}}$ (R_{conf} is the confinement radius, and $p_T \approx 0.4$ GeV).

The power-law corrections of the nucleon mass scale, which have a kinematic nature, are taken into account in (34) by means of the ξ-scaling formalism,[61] which predicts scaling with respect to the variable

$$\xi = 2x/(1+\sqrt{1+4x^2M_N^2/Q^2}).$$

In Refs. 61 and 62, systematic use of the equations of motion of the quarks in the gluon field and the application of dimensional analysis to the matrix elements of the operators of higher twists yielded the estimate

$$|B_{n,k}(Q^2)/A_n(Q^2)| \approx 1 \quad (35)$$

for all n, k, Q^2. Here, $A_n(Q^2)$ are the moments of the theoretical structure functions

$$A_n(Q^2) = \int_0^1 d\xi\xi^n F^{(\mathrm{th})}(\xi, Q^2). \quad (36)$$

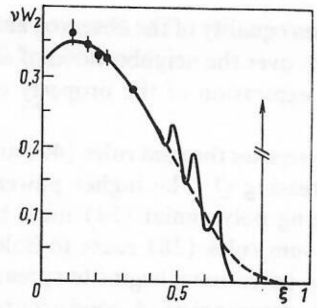

FIG. 6. Illustration of duality. The continuous curve is the result of fitting the SLAC experimental data[62]; the broken curve is the theoretical structure function $F^{(\mathrm{th})}$; the arrow indicates the elastic peak.

Using the estimate (35), we rewrite the relation (34) in the form

$$\int_0^1 d\xi\,\xi^n \left(F(\xi, Q^2) - F^{(\mathrm{th})}(\xi, Q^2)\right) = A_n(Q^2)\sum_{k=1}^{\infty}\left(n\frac{M_0^2}{Q^2}\right)^k. \quad (37)$$

From this we obtain a series of finite-energy sum rules

$$\int_{\xi_m}^1 d\xi\,\xi^n \left(F(\xi, Q^2) - F^{(\mathrm{th})}(\xi, Q^2)\right) \approx 0 \quad \text{for} \quad n \ll Q^2/M_0^2. \quad (38)$$

The cutoff ξ_m at the lower limit of integration is introduced here to reflect the early onset of scaling with respect to the variable ξ for $\xi < \xi_m$ (nonresonance region). The sum rules (38) express the property of global duality: In the resonance region, the smooth theoretical curve $F^{(\mathrm{th})}$ corresponding to the contribution of the Wilson operators of twist $\tau=2$ averages the physical structure function F, which oscillates around it (Fig. 6).

The sum rules (38) can also be used to explain the local duality found by Bloom and Gilman in deep inelastic lepton–nucleon interactions. Applying the sum rules (38) to each term of the localizing polynomial $\mathscr{P}$, which to the given accuracy has the property [Fig. 7(a)]

$$\mathscr{P}(\xi|\xi_+, \xi_-) = \sum_n a_n\xi^n \approx \theta(\xi-\xi_+)\,\theta(\xi_- - \xi), \quad \xi_- > \xi_+, \quad (39)$$

where $\xi_\pm$ are the limits of some resonance peak, we can write[16]

$$\int_{\xi_m}^1 d\xi\,\mathscr{P}(\xi|\xi_+, \xi_-)\left(F(\xi, Q^2) - F^{(\mathrm{th})}(\xi, Q^2)\right)$$
$$= \int_{\xi_+}^{\xi_-} d\xi\left(F(\xi, Q^2) - F^{(\mathrm{th})}(\xi, Q^2)\right) \approx 0. \quad (40)$$

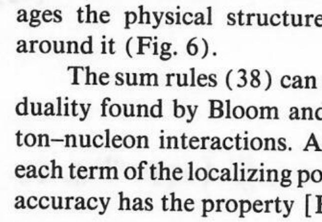

FIG. 7. Profiles of localizing polynomials.

This relation, which establishes equality of the observed and theoretical structure functions over the neighborhood of an individual resonance, is the expression of the property of local duality.

However, for practical purposes the sum rules (40) are of little use, since with decreasing Q^2 the higher powers $(n \sim Q^2/M_0^2)$ of the localizing polynomial (39) must be rejected, since for them the sum rules (38) cease to hold. Because of this, the localizing polynomial begins to spread, and the relations (40) become meaningless. A good accuracy can be expected from the sum rules only for $Q^2 \gtrsim Q_p^2 \gg M_0^2$. According to the estimates of Ref. 16, $Q_p^2 \sim 30\ \mathrm{GeV}^2$. Thus, the region that is most interesting from the point of view of studying elastic and quasielastic interactions is not covered by our treatment.

An attempt to extend the region of applicability of the sum rules (38) and (40) was made in Ref. 16. To take into account in the structure functions $F^{(\mathrm{th})}$ the power-law corrections of large scale ($M_0 \sim p_T \sim 0.4$ GeV), which destroy the locality of the relations (40), a new scaling variable was introduced:

$$\bar{\xi} = \xi \left[1 + \frac{M_0^2}{Q^2} \left(1 + \frac{M_0^2}{Q^2 + M_0^2} \right) \right]. \tag{41}$$

It is readily verified that when the variable $\bar{\xi}$ is substituted in the sum rules (38) power-law corrections of scale M_0 that correctly reproduce the behavior of the power (in M_0^2/Q^2) series in (34) arise. Indeed, let us expand $F^{(\mathrm{th})}(\bar{\xi}, Q^2)$ in powers of M_0^2/Q^2:

$$\tilde{F}^{(\mathrm{th})}(\xi, Q^2) = F^{(\mathrm{th})}(\xi, Q^2) + \frac{M_0^2}{Q^2}\, \xi\, \frac{\partial F^{(\mathrm{th})}(\xi, Q^2)}{\partial \xi} + O\left(\frac{M_0^4}{Q^4} \right) \tag{42}$$

and calculate the moments

$$\int_0^1 d\xi\, \xi^n F^{(\mathrm{th})}(\bar{\xi}, Q^2)$$
$$= \int_0^1 d\xi\, \xi^n F^{(\mathrm{th})}(\xi, Q^2) - (n+1) \frac{M_0^2}{Q^2} \int_0^1 d\xi\, \xi^n F^{(\mathrm{th})}(\xi, Q^2). \tag{43}$$

The second term in this expression is obtained after integrating by parts. Returning with allowance for this to the integration over ξ in (38), we find

$$\int_0^1 d\xi\, \xi^n \left(F(\xi, Q^2) - F^{(\mathrm{th})}(\xi, Q^2) \right)$$
$$= A_n(Q^2) \left(1 - (n+1) M_0^2/Q_2 + O(M_0^4/Q^4) \right). \tag{44}$$

In the general case, making analogous calculations, we can show that the coefficient of $(M_0^2/Q^2)^k$ is proportional to n^k $(n \gg 1)$. This agrees with the characteristic n dependence of the series on the right-hand side of (34) and shows that the introduction of the new scaling variable $\bar{\xi}$ correctly models the contribution of the power-law corrections $(M_0^2/Q^2)^k$. Moreover, the contribution of the twist-4 operators exactly corresponds to the result obtained in Refs. 61 and 63 on the basis of QCD.

Thus, by means of the variable $\bar{\xi}$ it is possible to take into account phenomenologically the power-law corrections of the large scale $\sim M_0$ and, as a result of this, we can expect a significant improvement in the local properties of the sum rules (40).

Note that in integrating over the neighborhood of an individual resonance in (40) we assume a correspondence in the normalizations of the resonance excitation form factor and the structure function $F^{(\mathrm{th})}$. In the general case, such correspondence is poorly justified. Sum rules that take into account explicitly the possible difference between the normalizations of the form factors and $F^{(\mathrm{th})}$ can be readily obtained from the sum rules (38) by using the localizing polynomial whose profile is shown in Fig. 7(b). Because of the narrowness of the "normalization" peak of height $1/Z$, situated opposite the peak of the resonance, and also with allowance for the smoothness of $F^{(\mathrm{th})}$, we obtain[16]

$$\int_{\xi_m}^1 d\xi\, \mathcal{P}_Z(\xi \mid \xi_+, \xi_-)\, F(\xi, Q^2) = \int_{\xi_-}^{\xi_+} d\xi F^{(\mathrm{th})}(\xi, Q^2). \tag{45}$$

This sum rule can be used to calculate the factors of electroweak resonance excitation, the normalization constant Z being assumed to be universal for all resonances.

It should be emphasized that the arguments given above in the derivation of the sum rules (45), just as in the derivation of the relations (40), do not possess predictive power. They merely make it possible to understand the position of these sum rules and the local duality which they express in the framework of QCD. One of the criteria for validity of the sum rules (45) could be comparison of the theoretical results obtained on their basis with experimental data on lepton–nucleon scattering.

5. DUAL QCD APPROACH TO THE DESCRIPTION OF TWO-PARTICLE LEPTON–NUCLEON PROCESSES

The study of Ref. 16 develops an approach to the calculation of structure functions (form factors) of two-particle lepton–nucleon processes based on perturbative QCD and the concept of local duality. For the mathematical formulation of the latter, the sum rules (45) are used.

We present the scheme of the dual QCD approach.

Restricting ourselves to the approximation of zero width ($\Gamma_R = 0$), we write down the resonance components of the physical structure functions in the neighborhood of a resonance R of mass M_R in the form

$$\left. \begin{aligned} F_1^R(\nu, Q^2) &= \overline{W}_1^R(Q^2)\, \delta(\nu - \nu_R); \\ F_{2,3}^R(\nu, Q^2) &= \nu \overline{W}_{2,3}^R(Q^2)\, \delta(\nu - \nu_R)/2M_N, \end{aligned} \right\} \tag{46}$$

where $\nu_R = (M_R^2 - M_N + Q^2)/2M_N$, and $\overline{W}^R(Q^2)$ are the required structure functions for production of the resonance R.

Besides the resonance component, the structure functions may contain an appreciable background admixture not associated with the production of resonances. We then face the problem of separating the resonance component from the physical structure functions F that occur on the left-hand side of the sum rules (45). Following Bloom and Gilman,[60] we attempt to solve this problem by generalizing the well-known ideas about the two-component nature of the scattering amplitude of strongly interacting particles[64] to lepton–nucleon processes. According to these ideas, the resonance component of the amplitude is associated with t-channel exchange of nonsinglet Regge trajectories, whereas the background component is associated with exchange of the Pomeranchuk trajectory. Regge analysis of the structure functions of deep inelastic scattering[60,65] indicates a direct connection between the nonsinglet (valence) part of the structure functions and the nonsinglet Regge trajectories in the t channel of virtual Compton scattering by the nucleon, while the singlet (sea) part is connected with the Pomeranchuk trajectory. It is this that is the justification for associating the resonance components of the physical structure functions F^R with the nonsinglet parts of the corresponding theoretical functions $F^{(\text{th})\text{NS}}$ and the background components with the singlet parts.

Applying this method of separation, we write down the sum rules (45) for the resonance structure functions:

$$\int_{\bar{\xi}_+}^{\bar{\xi}_-} d\bar{\xi}\mathscr{P}_Z(\bar{\xi}\,|\,\bar{\xi}_+,\ \bar{\xi}_-)\,F_k^R(\bar{\xi},\ Q^2)=\int_{\bar{\xi}_+}^{\bar{\xi}_-} d\bar{\xi}\,\bar{\xi}^{1-\delta_{2k}}F_k^{(\text{th})NS}(\bar{\xi},\ Q^2) \tag{47}$$

($k=1,2,3$). Substituting here (46) and taking into account the properties of the localizing polynomial $\mathscr{P}_z$ [Fig. 7(b)], we obtain

$$\overline{W}_k^R(Q^2)=ZT_k(Q^2)\int_{\bar{\xi}^+(Q^2)}^{\bar{\xi}^-(Q^2)} d\bar{\xi}\,\bar{\xi}^{1-\delta_{2k}}F_k^{(\text{th})NS}(\bar{\xi},\ Q^2), \tag{48}$$

where

$$\left.\begin{aligned} &T_1^R(Q^2)=\frac{\sqrt{\nu_R^2+Q^2}}{\bar{\xi}_R^2(Q^2)};\quad T_2^R(Q^2)=\frac{2M_N\sqrt{\nu_R^2+Q^2}}{\nu_R\bar{\xi}_R(Q^2)};\\ &T_3^R(Q^2)=\frac{2M_N\sqrt{\nu_R^2+Q^2}}{\nu_R\bar{\xi}_R^2(Q^2)}; \end{aligned}\right\} \tag{49}$$

$$\left.\begin{aligned} &\nu_R^{\pm}=((M_R\pm\Delta_R)^2-M_N^2+Q^2)/(2M_N);\\ &\bar{\xi}_R(Q^2)=\bar{\xi}(\nu_R,\ Q^2);\ \bar{\xi}_R^{\pm}(Q^2)=\bar{\xi}(\nu_R^{\pm},\ Q^2). \end{aligned}\right\} \tag{50}$$

Here, Δ_R is the width taken around the resonance peak, a quasifree parameter bounded by the distance to the nearest neighboring resonance.

The resonance structure functions (form factors) determined by (48) do not contain singular points in the region of spacelike momentum transfers, this being due to a property of the variable $\bar{\xi}$: $\bar{\xi}_R(Q^2=0)=\text{const}>0$. The variables ξ and x' do not have this property [$\xi_R(Q^2=0)=x'_R(Q^2=0)=0$], and if they are used, the form factors acquire an unphysical singularity at $Q^2=0$.

We represent the structure functions $E_k^{(\text{th})\text{NS}}$ in the form of a sum over the partial structure functions of the elementary transitions of the valence quarks $q_i\to q_f$, taking into account only transitions to the quark composition of the considered resonance:

$$F_k^{(\text{th})NS}(\bar{\xi},\ Q^2)=\sum_{i\to f}F_{i,f,k}^V(\bar{\xi},\ Q^2). \tag{51}$$

The partial structure functions $F_{if,k}^V$ for the ($V-A$) current of the quark transitions

$$j_\mu^{if}=\bar{q}_f\gamma_\mu(C_{if}^V+\gamma_5C_{if}^A)\,q_i \tag{52}$$

(C_{if}^V and C_{if}^A are the vector and axial coupling constants) have in the second order of perturbation theory the form

$$F_{if,k}^V(x,\ Q^2)=\mathscr{F}_{if,k}(x,\ Q^2)+\frac{\bar{g}^2(Q^2)}{16\pi^2}\times\int_x^1\frac{dy}{y}\,\overline{B}_k^{NS}\left(\frac{x}{y},\ Q^2\right)\mathscr{F}_{if,k}(y,\ Q^2). \tag{53}$$

The running coupling constant $\bar{g}^2$ depends on the variable Q^2 as follows:

$$4\pi\bar{\alpha}_s(Q^2)=\bar{g}^2(Q^2)=\frac{16\pi^2}{\frac{25}{3}\ln\frac{Q^2}{\Lambda^2}},\quad \Lambda\sim 0.1\div 0.5\ \text{GeV}. \tag{54}$$

The convolution kernels $\overline{B}_k^{\text{NS}}$ are given in the Appendix. The quantities $\mathscr{F}_{if,k}$ can be calculated using the formulas of the parton model,

$$\mathscr{F}_{if,k}(x,\ Q^2)=\alpha_k^{if}f_V^{(i)}(x,\ Q^2)\,x^{\delta_{2k}}, \tag{55}$$

where

$$\alpha_k^{if}=(C_{if}^{V^2}+C_{if}^{A^2})(\delta_{1k}+\delta_{2k})-2C_{if}^VC_{if}^A\delta_{3k} \tag{56}$$

are the structure functions of a point quark, and $f_V^{(i)}$ are the distribution functions of the initial valence quarks in the nucleon, and they are subject to the QCD evolution equations [see (78)].

We emphasize the importance of taking into account the $\bar{g}^2$ corrections to the leading logarithmic approximation, i.e., to the leading term of perturbation theory, from the point of view of the group of problems considered here. Indeed, in the study of resonance phenomena the greatest interest attaches to the region of comparatively small Q^2 (of the order of several GeV), where these corrections are appreciable and must be taken into account.

The mass corrections due to the nonzero mass M_N of the target nucleon and the mass m_f of the quark formed in the elementary interaction event are taken into account by replacing the variable x in the parton formulas by $\bar{\xi}$. We ignore the mass of the active quark. We do not use the rigorous formulas of ξ scaling, since they become meaningless in the region $Q^2\sim M_N^2$. However, it is known[61] that in the region in which they are applicable almost the entire effect of taking into account the mass corrections reduces to this change of the variables. Therefore, the approximation which we have made is correct in a fairly wide range of momentum transfers Q^2.

The expression (53) can be rewritten nominally as

$$F_{if,k}^V(\bar{\xi},\ Q^2)=\alpha_k^{if}\hat{\eta}_k(f_V^{(i)}\,|\,\bar{\xi},\ Q^2), \tag{57}$$

where $\hat{\eta}_k(f_V^{(i)}|\bar{\xi},Q^2)$ is a symbolic expression for a block of expressions that do not depend on the parameters of the ($V-A$) transition. Substituting (57) in the sum rules (48), we obtain

$$\overline{W}_k^R(Q^2)=\sum_{i\to f}\alpha_k^{if}D_{i(k)}^R(Q^2); \tag{58}$$

$$D_{i(k)}^R(Q^2)=h_k^{R(1)}(Q^2)+\frac{\bar{g}^2(Q^2)}{16\pi^2}\,h_k^{R(2)}(Q^2); \tag{59}$$

$$h_k^{R(1)}(Q^2)=ZT_k^R(Q^2)\int_{\bar{\xi}_R^+(Q^2)}^{\bar{\xi}_R^-(Q^2)}dt\,f_V^{(i)}(t,\ Q^2)\,t; \tag{60}$$

$$h_k^{R(2)}(Q^2)=ZT_k^R(Q^2)\int_{\bar{\xi}_R^+(Q^2)}^{1}dt\,f_V^{(i)}(t,\ Q^2)\,t\times\int_{\bar{\xi}_R^+(Q^2)/t}^{1}dx\,x^{1-\delta_{2k}}B_k(x)\,\theta\left(\frac{\bar{\xi}_R^-(Q^2)}{t}-x\right). \tag{61}$$

From this it is readily seen that we have essentially arrived at a partonlike picture of the two-particle lepton–nucleon processes: Scattering takes place on a point quark–parton, after

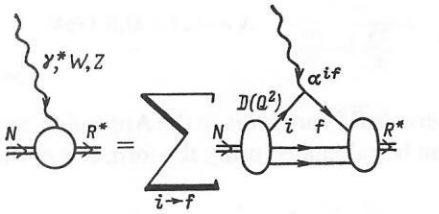

FIG. 8. Diagram of a two-particle lepton–nucleon process and parton prescription for its calculation.

which the quark that has interacted recombines with two spectator quarks into the given baryon resonance. Here, the quark factor $D^R_{(i,k)}$ plays the part of the parton distribution function. It is the integral transform of the distribution function of the valence quark of type i. A test of the recombination process is realized by the mass M_R of the resonance and the width $D^R_{i(k)}$ taken around it, which occur in Δ_R. In addition, the functions $D^R_{i(k)}$ contain hypothetical information about large distances (the dependence on $M_0 \sim p_T$). An illustration of what we have said is Fig. 8, which also gives a clear diagrammatic prescription for calculating the structure functions $\overline{W}^R_k$ of the resonance processes.

When Eqs. (58)–(61) are used in the region of small $Q^2(Q^2 \sim p_T^2)$, we shall replace Q^2 by $Q^2 + p_T^2$ in $f_V^{(i)}(\xi, Q^2)$ and $\overline{g^2}(Q^2)$. This replacement is due to the circumstance that the gluons within the nucleon cannot, by virtue of the uncertainty principle, have zero momentum, and its mean value is $p_T \sim 1/R_{\text{conf}}$. Therefore, in all QCD interactions leading to the violation of scaling (to a Q^2 dependence in $f_V^{(i)}$), the gluons participate with momentum $Q^2 + p_T^2$ and not Q^2. It is this that provides the justification for the foregoing substitution, which in essence is a manifestation of the well-known "freezing" of the quark–gluon coupling constant, which is expressed by $\overline{g^2}(Q^2 \to 0) = \overline{g^2}(p_T^2) \neq 0$.

In the dual approach, the asymptotic behavior of the form factors as $Q^2 \to \infty$ is determined by the behavior of the quark distributions $f_V^{(i)}(\xi, Q^2)$ in the limit $x \to 1$, i.e., by a configuration of the quarks in which one of them carries the entire gluon momentum. Thus, the dual QCD approach gives a certain realization of Feynman's well-known mechanism[66] in QCD.

We consider in more detail the asymptotic behavior of the nucleon form factors $F^N(Q^2)$ in the given case. Our point of departure is the QCD prediction for the threshold behavior of the structure functions [68,69]:

$$f_V(x, Q^2) \xrightarrow[x \to 1]{} (1-x)^{\widetilde{\tau}(Q^2)}, \tag{62}$$

where $\widetilde{\tau}(Q^2) = \text{const} + (4C_F/b)s$, $C_F = 4/3$, $b = 11 - (2/3)n_f$, and n_f is the number of quark flavors. Substituting (62) in (58)–(61) and bearing in mind that $a + (Q^2) \underset{Q^2 \to \infty}{\to} 1$, we find from the asymptotic estimate of the integral

$$F^N(Q^2) \sim \sqrt{\overline{W}_k} \xrightarrow[Q^2 \to \infty]{} \exp\left[-\frac{2C_F}{b} \ln(\ln Q^2) \ln Q^2\right]. \tag{63}$$

As was to be expected, we obtain the rapid decrease characteristic of the Sudakov form factor[70] with increasing Q^2. This means that the asymptotic behavior of the form factor is determined not by the Feynman mechanism but by the hard-rescattering mechanism. The latter gives only a power-law decrease for the form factors. But in the region of moderate Q^2, as was pointed out in Sec. 3, the contribution of the hard-rescattering mechanism is suppressed, and the situation is reversed.

The structure functions α_k^{if} of transitions of point quarks for the electromagnetic interaction are determined by the squares of the electric charges of the quarks, and in the case of the weak interactions by the structure of the weak charged current in the GIM model[67]:

$$\begin{aligned} J_\mu^{CC} &= \bar{u}\gamma_\mu (1+\gamma_5)(d \cos\theta_C + s \sin\theta_C) \\ &+ \bar{c}\gamma_\mu (1+\gamma_5)(s \cos\theta_C - d \sin\theta_C) \end{aligned} \tag{64}$$

and by the structure of the neutral current (3) in the Weinberg–Salam model.

As an example, we consider a number of two-particle lepton–nucleon processes, for which Fig. 9 gives the quark diagrams corresponding to the parton prescription for calculating the structure functions in the dual QCD approach. The electromagnetic processes are described by two structure functions:

$$\overline{W}^{R,\,em}_{1,\,2}(Q^2) = D^R_{d(1,\,2)}(Q^2). \tag{65}$$

The two-particle processes due to interactions with the weak charged current are characterized by the structure functions

$$\begin{aligned} &\overline{W}^{\Delta^{++}}_{1,\,2}(Q^2) = 2\cos^2\theta_C D^{\Delta^{++}}_{d(1,\,2)}(Q^2), \\ &\overline{W}^{\Delta^{++}}_{3}(Q^2) = 2\cos^2\theta_C D^{\Delta^{++}}_{d(3)}(Q^2); \\ &\overline{W}^{R,\,CC}_{1,\,2}(Q^2) = 4\cos^2\theta_C D^{R,\,CC}_{d(1,\,2)}(Q^2); \\ &\overline{W}^{R,\,CC}_{3}(Q^2) = -4\cos^2\theta_C D^{R,\,CC}_{d(3)}(Q^2); \\ &\overline{W}^{C_1^{++}}_{1,\,2}(Q^2) = 2\sin^2\theta_C D^{C_1^{++}}_{d(1,\,2)}(Q^2); \\ &\overline{W}^{C_1^{++}}_{3}(Q^2) = -2\sin^2\theta_C D^{C_1^{++}}_{d(3)}(Q^2); \\ &\overline{W}^{C_0^{+}}_{1,\,2}(Q^2) = 4\sin^2\theta_C D^{C_0^{+}}_{d(1,\,2)}(Q^2); \\ &\overline{W}^{C_0^{+}}_{3}(Q^2) = -4\sin^2\theta_C D^{C_0^{+}}_{d(3)}(Q^2). \end{aligned} \tag{66}$$

For the two-particle processes due to the interactions with the weak neutral current the structure functions have the form

$$\begin{aligned} &\overline{W}^{R_1,\,NC}_{1,\,2}(Q^2) = \left(\frac{3}{2} - \frac{10}{3}x + 4x^2\right) D^{R_1}_{d(1,\,2)}(Q^2); \\ &\overline{W}^{R_1,\,NC}_{3}(Q^2) = -\left(\frac{3}{2} - \frac{10}{3}x\right) D^{R_1}_{d(3)}(Q^2); \\ &\overline{W}^{R_2,\,NC}_{1,\,2}(Q^2) = \left(\frac{3}{2} - \frac{8}{3}x + \frac{24}{9}x^2\right) D^{R_2}_{d(1,\,2)}(Q^2); \\ &\overline{W}^{R_2,\,NC}_{3}(Q^2) = -\left(\frac{3}{2} - \frac{8}{3}x\right) D^{R_2}_{d(3)}(Q^2), \end{aligned} \tag{67}$$

where $x = \sin^2\theta_W$.

We use these results to describe the experimental data and elucidate some problems relating to the experimental status of QCD.

6. ANALYSIS OF EXPERIMENTAL DATA

To show that the dual QCD approach can be used to describe two-particle lepton–nucleon processes, we consider quasielastic and elastic lepton–nucleon scattering in the leptoproduction of the isobar Δ_{33} ($ep \to e\Delta^+$, $\nu_\mu p \to \mu^-\Delta^{++}$).

The weak and electromagnetic form factors of lepton–

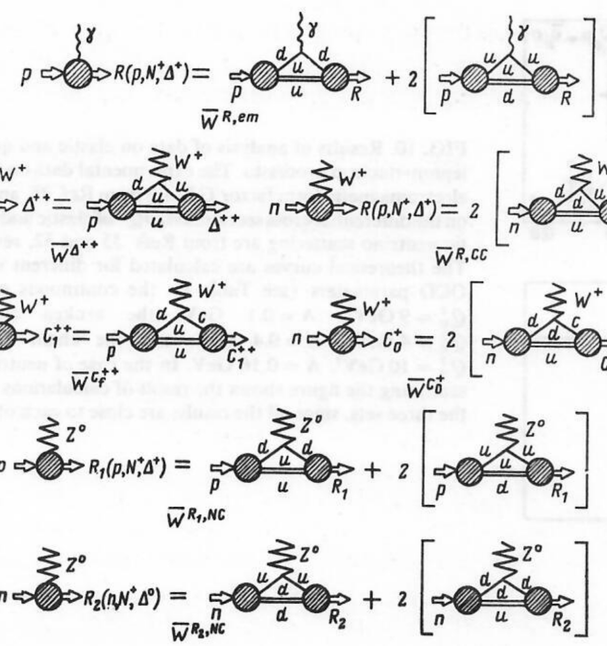

FIG. 9. Examples of the application of the parton prescription for calculations to calculation of the structure functions of two-particle lepton–nucleon processes.

nucleon scattering are related to the resonance structure functions $\overline{W}_2^{em}$ and $\overline{W}_2^{w}$ by

$$\overline{W}_2^{em}(Q^2) = 2M_N\left((G_E^p)^2 + \frac{Q^2}{4M_N^2}(G_M^p)^2\right)/\tau,$$
$$\overline{W}_2^{w}(Q^2) = 2M_N\left(F_V^2 + \frac{Q^2}{4M_N^2}F_M^2\right) + 2M_N F_A^2. \quad (68)$$

Using Eqs. (2)–(5), we obtain

$$F_V^{CC} = P_V(Q^2)\sqrt{\overline{W}_2^{em}};\quad F_M^{CC} = P_M(Q^2)\sqrt{\overline{W}_2^{em}};$$
$$F_A^{CC} = \left[\frac{1}{2M_N}\overline{W}_2^{w} - \left(P_V^2(Q^2) + \frac{Q^2}{4M_N^2}P_M^2(Q^2)\overline{W}_2^{em}\right)\right]^{1/2};$$
$$F_{V,M}^{NC} = \frac{1}{2}F_{V,M}^{CC} - 2\sin^2\theta_W \overline{P}_{V,M}(Q^2)\sqrt{\overline{W}_2^{em}};$$
$$F_A^{NC} = \frac{1}{2}F_A^{CC}. \quad (69)$$

Here

$$P_M(Q^2) = (\mu_p - \mu_n - 1)\,S(Q^2),$$
$$P_V(Q^2) = \left(1 + \frac{Q^2}{4M_N^2}(\mu_p - \mu_n)\right)S/Q^2);$$
$$\overline{P}_M(Q^2) = \left(1 + \frac{Q^2}{4M_N^2}\mu_p\right)S(Q^2), \quad (70)$$
$$\overline{P}_V(Q^2) = (\mu_p - 1)\,S(Q^2);$$
$$S(Q^2) = \left[2M_N\left(1 + \frac{\mu_p^2 Q^2}{4M_N^2}\right)\tau\right]^{-1/2}.$$

In the framework of the dual approach, the structure functions $\overline{W}_2^{em}$ and $\overline{W}_2^{w}$ have the form

$$\overline{W}_2^{em} = D_{d(2)}(Q^2),\quad \overline{W}_2^{w} = 4\cos^2\theta_C D_{d(2)}(Q^2). \quad (71)$$

TABLE I. Results of analysis of experimental data in the dual approach.

Q_0^2, GeV^2	Λ, GeV	b_0	b_1	β_0	β_1	τ_0	Z_N	p_T, GeV
9	0.1	0.992	0.62	2.23	0.995	1.97	2.04 ± 0.06	0.38 ± 0.01
4	0.4	0.96	0.53	2.81	0.79	1.51	1.44 ± 0.05	0.449 ± 0.008
10	0.16	1.46	1.17	1.99	0.51	2.07	$2.94^{+0.15}_{-0.05}$	$0.431^{+0.004}_{-0.010}$

It is convenient to represent the expressions (59)–(61) for the quark factor $D_{d(2)}(Q^2)$ in the form

$$D_{d(2)}(Q^2) = h^{(1)}(Q^2) + \frac{\overline{g}^2(\hat{Q}^2)}{16\pi^2}h^{(2)}(Q^2);$$
$$h^{(1)}(Q^2) = Z_N T(Q^2)\int_{a_+}^{1} dt\, f_V(t, \hat{Q}^2)\, t\theta(1-t);$$
$$h^{(2)}(Q^2) = Z_N T(Q^2)\int_{a_+}^{1} dt\, f_V(t, \hat{Q}^2)\, t\theta(1-t)\int_{a_+/t}^{1} dx\, B_2(x);$$
$$\hat{Q}^2 = Q^2 + p_T^2; \quad (72)$$
$$T(Q^2) = \frac{M_N}{K(Q^2)}\left[1 + \frac{4M_N^2}{Q^2} + \sqrt{1 + \frac{4M_N^2}{Q^2}}\right];$$
$$K(Q^2) = 1 + \frac{p_T^2}{Q^2}\left(1 + \frac{1}{1 + Q^2/p_T^2}\right);$$
$$a_+(Q^2) = \frac{Q^2 K(Q^2)}{M_N(\nu_+ + \sqrt{\nu_+^2 + Q^2})};$$
$$\nu_+ = \frac{(M_N + \Delta_N)^2 + M_1^2 + Q^2}{2M_N}.$$

The normalization constant Z_N is a free parameter, and the width Δ_N taken around the nucleon peak is a bounded parameter ($0 \leqslant \Delta_N \leqslant 0.29$ GeV).

The distribution functions $f_V(t,Q^2)$ of the valence quarks satisfy the QCD evolution equations. Specifying the initial conditions, for example, in the framework of the QCD parton model with Regge asymptotic behavior,[54,55] we can obtain to within a 3%–5% error solutions of these equations in explicit form:

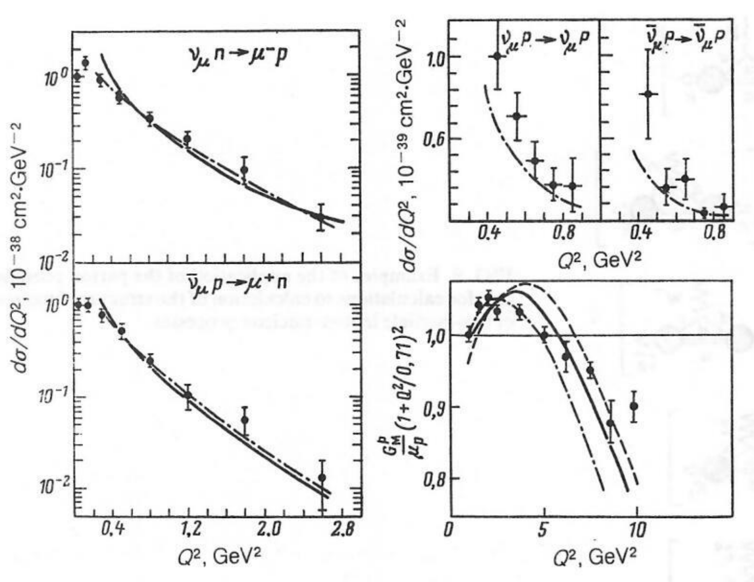

FIG. 10. Results of analysis of data on elastic and quasielastic lepton–nucleon processes. The experimental data on the proton electromagnetic form factor G_M^p are from Ref. 25, and the data on the differential cross sections $d\sigma/dQ^2$ of elastic and quasielastic neutrino scattering are from Refs. 35 and 32, respectively. The theoretical curves are calculated for different sets of the QCD parameters (see Table I): the continuous curve with $Q_0^2 = 9$ GeV², $\Lambda = 0.1$ GeV, the broken curve with $Q_0^2 = 4$ GeV², $\Lambda = 0.4$ GeV, and the chain curve with $Q_0^2 = 10$ GeV², $\Lambda = 0.16$ GeV. In the case of neutrino elastic scattering the figure shows the result of calculations for one of the three sets, since all the results are close to each other.

$$f_V(t,\ Q^2) = \frac{t^{-1/2}(a-t)^{\tilde\tau(Q^2)}}{B(1/2,\tilde\tau(Q^2)+1)}\ \frac{\Phi(b(Q^2),\ \tilde\tau(Q^2)+1;\ \beta(Q^2)(1-t))}{\Phi(b(Q^2),\ \tilde\tau(Q^2)+3/2;\ \beta(Q^2))}, \tag{73}$$

where $B(a,b) = \Gamma(a)\Gamma(b)/\Gamma(a+b)$ is the beta function, and

$$\Phi(\alpha,\ \beta;\ z) = \sum_{k=0}^{\infty} \frac{z^k}{k!}\ \frac{\Gamma(\alpha+k)\,\Gamma(\beta)}{\Gamma(\alpha)\,\Gamma(\beta+k)};$$

$$\tilde\tau(Q^2) = \tau_0 + \tau_1 s;\ b(Q^2) = b_0 + b_1 s;\ \beta(Q^2) = \beta_0 + \beta_1 s;$$

$$s = \ln\left(\frac{\ln \hat Q^2/\Lambda^2}{\ln Q_0^2/\Lambda^2}\right). \tag{74}$$

Here, Q_0^2 is the normalization point, $\tau_1 = 0.64$, and the QCD parameters $\tau_0, b_0, b_1, \beta_0, \beta_1$ are determined using the data on deep inelastic lepton–nucleon scattering[54] (see Table I).

In Ref. 18 data[25] on the proton electromagnetic form factor G_M^p and the differential cross sections $d\sigma/dQ^2$ of quasielastic[32] and elastic[35] neutrino and antineutrino scattering were analyzed in the framework of the dual approach. The free parameters in the analysis were the normalization constant Z_N and the mean transverse momentum p_T of a quark in the nucleon. The duality interval was chosen to be maximal: $\Delta_N = 0.29$ GeV. For the QCD parameters of the quark distributions in the nucleon, $\tau_0, b_0, b_1, \beta_0, \beta_1$, the values obtained for different Q_0^2 and Λ from analysis of data on deep inelastic lepton–nucleon scattering[54,71] were taken. Table I and Fig. 10 give the results only for three sets of variables $Q_0^2, \Lambda, \tau_0, b_0, b_1, \beta_0, \beta_1$, these giving the best description of the experimental data on the elastic and quasielastic lepton–nucleon scattering. Altogether, eight variants of solutions obtained using the analysis of the deep inelastic scattering were analyzed. It can be seen from Fig. 10 that the best description of the experimental data is obtained for values of the QCD parameters corresponding to the variant with $Q_0^2 = 10$ GeV² and $\Lambda = 0.16$ GeV (last row of the table). It is possible to reproduce not only qualitatively but also quantitatively the deviation of the proton electromagnetic form factor G_M^p from the dipole parametrization in the region $Q^2 \lesssim 5$ GeV². Note that the constant Z_N gives the absolute normalization of the differential cross section, whereas the slope of the function $\log(d\sigma/dQ^2)$ is completely determined by the mean transverse quark momentum p_T in the nucleon. The difference between the calculated and experimental differential cross sections $d\sigma/dQ^2$ for elastic $\nu(\bar\nu)N$ scattering can be attributed to the presence of a systematic error due to the complexity of the normalization of the differential cross sections $d\sigma/dQ^2$ and the neutrino spectra.

The electroproduction and neutrino-induced production reactions are described by the structure functions $\overline{W}_{1,2}^{\Delta,\mathrm{em}}$ and $\overline{W}_{1,2,3}^{\Delta^{++}}$, respectively. The invariant structure functions $\overline{W}_{1,2}^{\Delta,\mathrm{em}}$ (65) are related to the helicity amplitudes $f_{\pm 0}$ [see (24)] by

$$\overline{W}_1^{\Delta,em}(Q^2) = \frac{M_\Delta^2}{M_N}(|f_+|^2 + |f_-|^2);$$

$$\overline{W}_2^{\Delta,em}(Q^2) = M_N\left[2\left(\frac{Q^2}{\tilde Q^2}\right)|f_0|^2 + \frac{|Q^2|}{\tilde Q^2}(|f_+|^2 + |f|^2)\right]. \tag{75}$$

From (25), taking into account the dominance of the M_1 transition in the $ep \to e\Delta^+$ reaction, we obtain a simple connection between the form factor $G_{M\Delta}$ (25) and the structure function $\overline{W}_2^{\Delta,\mathrm{em}}$

$$G_{M\Delta}^2(Q^2) = \frac{M_N}{|Q^2|}\overline{W}_2^{\Delta,em}(Q^2). \tag{76}$$

In Ref. 18, an analysis was made of the data[46] on the form factor $G_{M\Delta}$ and the differential cross section $d\sigma/dQ^2$ of the $\nu_\mu\, p \to \mu^-\Delta^{++}$ reaction,[51] which was expressed in terms of the invariant structure functions $\overline{W}_{1,2,3}^{\Delta^{++}}$ (66) as follows:

$$\frac{d\sigma}{dQ^2}(E_\nu) = \frac{G^2}{2\pi}\left\{\left(1 - \frac{\nu_\Delta}{E_\nu} - \frac{Q^2}{2E_\nu^2}\right)\frac{1}{2M_N}\overline{W}_2^{\Delta^{++}}(Q^2) + \frac{Q^2}{4M_N E_\nu^2}\overline{W}_1^{\Delta^{++}}(Q^2) - \left(1 - \frac{\nu_\Delta}{2E_\nu}\right)\frac{Q^2}{4M_N^2 E_\nu}\overline{W}_3^{\Delta^{++}}(Q^2)\right\}, \tag{77}$$

where $\nu_\Delta = \nu_R\,|_{M_R = M_\Delta}$.

For the analysis of the data on the electroproduction and neutrino-induced production of the Δ_{33} isobar use was also made of various sets of values of the QCD parameters

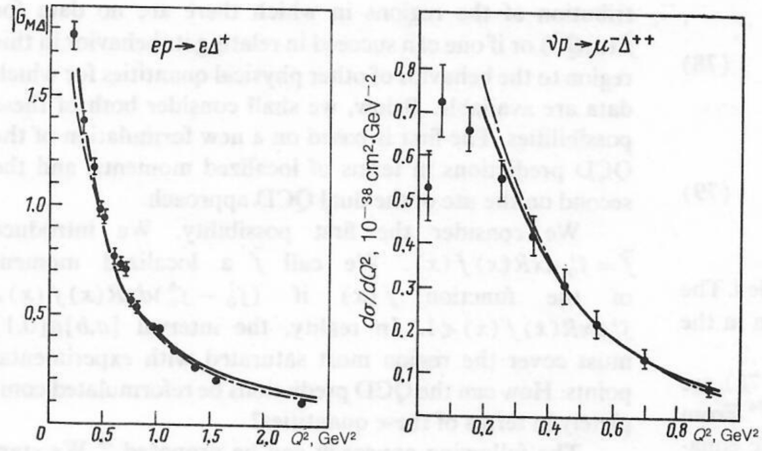

FIG. 11. Results of simultaneous analysis of experimental data on electroproduction and neutrino-induced production of the Δ_{33} isobar. The data on the $N\Delta$ transition form factor $|G_{M\Delta}|$ are taken from Ref. 46, and the data on the differential cross section $d\sigma/dQ^2$ of the $\nu_\mu p\to\mu^-\Delta^{++}$ reaction are from Ref. 51; the theoretical curves are the same as in Fig. 10.

obtained from deep inelastic scattering data.[54,71] For the duality interval, the value $\Delta_R = 0.2$ GeV was chosen. Figure 11 shows the results only for two sets of QCD parameter values, these giving the best description of the data on the electroproduction and neutrino-induced production of the Δ_{33} isobar and corresponding to the values $Q_0^2 = 9$ GeV^2, $\Lambda = 0.1$ GeV, and $Q_0^2 = 10$ GeV^2, $\Lambda = 0.16$ GeV (see Table I). For the parameter p_T in the first case we obtain $p_T = 0.42 \pm 0.01$ GeV, and in the second $p_T = 0.44 \pm 0.01$ GeV. In both cases, the normalization constant Z_R is found to be $Z_R = 1.0 \pm 0.1$.

Figure 12 shows the total cross section of the $\nu_\mu p\to\mu^-\Delta^{++}$ reaction as a function of the neutrino energy. Calculations in the dual QCD approach were made for the values of the parameters obtained in the variant of the analysis with $Q_0^2 = 10$ GeV^2 and $\Lambda = 0.16$ GeV. For comparison, the figure also shows the curve calculated in Adler's model.[52]

Combined analysis of all the experimental data given in Figs. 11 and 12 showed that the best description is obtained in the region $Q^2 \lesssim 5$ GeV^2 for the values of the QCD parameters corresponding to the variant with $Q_0^2 = 10$ GeV^2, $\Lambda = 0.16$ GeV. All the remaining variants must be rejected on the basis of the χ^2 test. The mean transverse quark momentum in the nucleon is found to be $p_T = 0.43 \pm 0.01$ GeV.

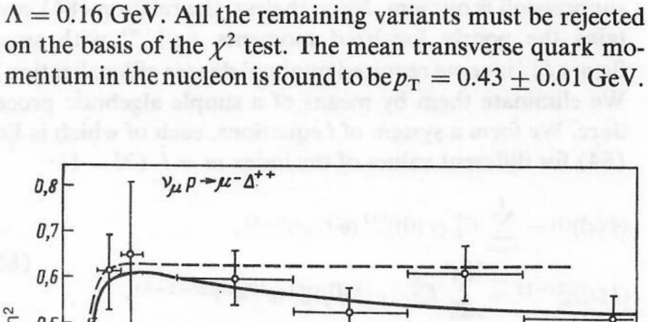

FIG. 12. Dependence of the $\nu_\mu p\to\mu^-\Delta^{++}$ reaction cross sections on the neutrino energy E_ν. Experimental points: the black circles [*sic*] are from Ref. 51, and the open circles from Ref. 49; the continuous curve represents the calculations in the dual approach, and the broken curve is the result in Adler's model.[52]

Thus, the analysis made in Ref. 18 of the experimental data shows that the dual QCD approach makes it possible to describe numerous two-particle lepton–nucleon processes and to obtain independent information about the quark–gluon structure of the nucleon. It has been shown that the parameter p_T that arises in the dual approach is universal for all elastic, quasielastic, and resonance processes, and this confirms the physical interpretation given to it of the mean transverse quark momentum in the nucleon. Our value $p_T = 0.43 \pm 0.01$ GeV agrees well with the generally accepted estimates of this parameter. We must also emphasize the fact that the use as additional information of the experimental data on the two-particle lepton–nucleon processes at moderate Q^2 significantly reduces the uncertainty in the determination of the parameters that characterize the quark distribution in the nucleon with respect to the longitudinal momentum. Such uncertainties are usual in the procedure of extracting the quark distributions and the QCD parameter Λ from the existing experimental data on deep inelastic lepton–nucleon scattering.

7. ON THE VALUE OF THE QCD PARAMETER Λ

Quantum chromodynamics is now firmly established as the theory of the strong interactions of elementary particles. There is at present no theory capable of seriously competing with QCD. And yet, what is its experimental status? How secure is it? In particular, do the QCD predictions agree with the extensive experimental data on deep inelastic scattering at our disposal? Unfortunately, the affirmative answer to the last question reflects the universal adherence to gauge theories rather than the real state of affairs. It would be more correct to say that a definitive and unambiguous answer has not yet been obtained. At the least, not a few very serious problems remain to be resolved. Below, we shall consider only one of them, namely, the model dependence of the results of comparison of the QCD predictions with experimental data. Such a dependence leads to significant uncertainties when the QCD parameter Λ is deduced from data. Let us explain the essence of the problem.

To this end, we recall the basic predictions of QCD for the structure functions $F_k(x,Q^2)$ of deep inelastic electron–nucleon scattering. We have here the evolution equation with respect to the variable Q^2. For simplicity, we consider only the evolution of the nonsinglet components of the structure functions $F_k^{NS}(x,Q^2)$ in the leading order in $\alpha_S(Q^2)$:

$$\frac{df(x,s)}{ds} = \int_x^1 \frac{dy}{y} P\left(\frac{x}{y}\right) f(y,s),$$
$$f(x,0) = f^{IC}(x), \tag{78}$$

where

$$f(x,s) = F_{1,3}(x,Q^2);\; F_2(x,Q^2)\,x; \tag{79}$$
$$s = \frac{2}{\beta_0} \ln \frac{\alpha_s(Q_0^2)}{\alpha_s(Q^2)};$$

Q_0^2 is the normalization point of the evolution variable s. The explicit form of the splitting function $P(x)$ is given in the Appendix.

The evolution equations written in the form (78) are known as the Lipatov–Altarelli–Parisi equations.[73,74] From these equations one can readily go over to algebraic equations for the moments $\langle f \rangle_n$ of the structure function $f(x,s)$:

$$\langle f(s) \rangle_n = \langle f^{IC} \rangle_n \, e^{\langle P \rangle_n s}; \tag{80}$$

in accordance with the definition

$$\langle f(s) \rangle_n \equiv \int_0^1 dx\, x^{n-1} f(x,s). \tag{81}$$

The two formulations of the QCD predictions in the form (78) and (80) are mathematically equivalent. To solve them, it is necessary to know the initial conditions $f^{IC}(x)$, i.e., the structure function at $Q^2 = Q_0^2$ $(s=0)$. But these cannot be calculated by perturbation theory and in the framework of QCD are still undetermined. We emphasize that uncertainties of this kind are due to the absence of adequate methods of working with QCD on the scales of the characteristic hadron dimensions. One way or another, to test the predictions it is necessary to specify $f^{IC}(x)$ and solve Eqs. (78) or (80). At this stage, it is necessary to use models that determine the form of this function phenomenologically. Thus, the results of comparing the QCD predictions with the experimental data depend on the type of model employed. Let us see whether this dependence is great and whether it can be eliminated or at least weakened.

It would seem that the answer is obvious. We shall not appeal to any model but directly choose a function $f^{IC}(x) = f(x,Q_0^2)$ that passes through the experimental points. In other words, we take it directly from the experimental data. However, such a procedure is not unique. Entirely different functions can pass equally well through the points but differ appreciably in the kinematic region in which there are no points. Therefore, in this approach one obtains not one but an entire class of functions. In principle, the class can be restricted by further experimental measurements. However, the arbitrariness cannot be completely eliminated. There are regions that for their own reasons are effectively removed from the experimental data. Such are the regions near the boundaries of the physical interval $x \in [0,1]$. Because of kinematic restrictions, experimental advance in the direction of the limit points $x \to 0$ and 1 is extremely difficult, to say nothing of the fact that the question of the asymptotic behavior of $f(x,Q^2)$ is experimentally unresolved. Thus, in such an approach a model dependence of the results of comparing the QCD predictions with the experimental data remains. This dependence can be ignored only in two cases—if the prediction does not contain a contribution of the regions in which there are no data for $f(x,Q^2)$ or if one can succeed in relating its behavior in this region to the behavior of other physical quantities for which data are available. Below, we shall consider both of these possibilities. The first is based on a new formulation of the QCD predictions in terms of localized moments, and the second on the use of the dual QCD approach.

We consider the first possibility. We introduce $\bar{f} = \int_0^1 dx R(x) f(x)$. We call $\bar{f}$ a localized moment of the function $f(x)$ if $(\int_0^1 - \int_a^b) dx R(x) f(x) / \int_0^1 dx R(x) f(x) \ll 1$. In reality, the interval $[a,b] \in [0,1]$ must cover the region most saturated with experimental points. How can the QCD predictions be reformulated completely in terms of these quantities?

The following approach can be proposed.[75] We start from Eq. (78). To both sides, we apply the integral transformation

$$\langle f \rangle_n^{(m)} = \int_0^1 dx\, x^{n-1} \ln^m x\, f(x). \tag{82}$$

Noting that

$$\frac{d^m \langle f \rangle_n}{dn^m} = \frac{d^m}{dn^m} \int_0^1 dx\, x^{n-1} f(x)$$
$$= \int_0^1 dx\, x^{n-1} \ln^m x\, f(x) = \langle f \rangle_n^{(m)}, \tag{83}$$

we obtain the relation

$$\langle f(s) \rangle_n^{(m)} = \sum_{k=0}^{m} C_n^k \langle f(0) \rangle_n^{(k)} (e^{\langle P \rangle_n s})^{(m-k)}. \tag{84}$$

The $\langle f \rangle_n^{(m)}$ here are auxiliary localized moments. The main contribution to the value of $\langle f \rangle_n^{(m)}$ is made by the region of integration near the point $x = m/(n-1)$. The undesirable contribution from the neighborhoods of the boundaries $x = 0$ and 1 of the physical region are suppressed more strongly, the larger are n and m. The introduction of this suppression is our aim. Nevertheless, the relation (84) contains the poorly localized moments $\langle f \rangle_n^{(m)}$ with small $0 \leqslant m \leqslant l$ (l is some required minimal degree of localization). We eliminate them by means of a simple algebraic procedure. We form a system of l equations, each of which is Eq. (84) for different values of the index $m = l$–$(2l-1)$:

$$\langle f(s) \rangle^{(l)} = \sum_{k=0}^{l} C_l^k \langle f(0) \rangle_n^{(k)} (e^{\langle P \rangle_n s})^{(l-k)},$$
$$\langle f(s) \rangle_n^{(2l-1)} = \sum_{k=0}^{2l-1} C_{2l-1}^k \langle f(0) \rangle_n^{(k)} (e^{\langle P_n \rangle s})^{(2l-1-k)}. \tag{85}$$

Using this system, we express the l poorly localized moments $\langle f(0) \rangle_n^{(k)}$ with indices $k = 0$–$(l-1)$ in terms of the strongly localized moments $\langle f(s) \rangle_n^{(k)}$, $\langle f(0) \rangle_n^{(k)}$ with indices $k \geqslant l$. We substitute these expressions in (84) with $m = 2l$. We obtain the equation

$$\langle f(s) \rangle_n^{(2l)} - \sum_{k=l}^{2l-1} R_n^{l,k}(s) \langle f(s) \rangle_n^{(k)} =$$
$$= \left[\langle f(0) \rangle_n^{(2l)} - \sum_{k=l}^{2l-1} R_n^{l,k}(-s) \langle f(0) \rangle_n^{(k)} \right] e^{\langle P \rangle_n s}. \tag{86}$$

It does not contain poorly localized moments. The explicit form of $R_n^{l,k}(s)$, which are linear-rational functions of s, is given in Ref. 75. It is convenient to rewrite the relation (86) in the form

$$\int_0^1 dx\, R_n^l(x,\ s) f(x,\ s) = \int_0^1 dx\, Q_n^l(x,\ s) f(x,\ 0), \qquad (87)$$

where

$$R_n^l(x,\ s) = x^{n-1}\left[\ln^{2l} x - \sum_{k=l}^{2l-1} \ln^k x R_n^{l,k}(s)\right],$$
$$Q_n^l(x,\ s) = R_n^l(x,\ -s)\, e^{\langle P\rangle_n s}. \qquad (88)$$

The main contribution to Eq. (87) is made by the interval of integration $e^{-2l/(n-1)} \leqslant x \leqslant e^{-l/(n-1)}$. By appropriate choice of l and n we can separate any interval in which we are interested within the physical region of x. Figure 13 gives a graph that represents the algorithm for this choice, and Fig. 14 shows the form of the functions $R_n^l(x,s)$ and $Q_n^l(x,s)$ for some values of n, l, and s.

Thus, we have formulated the QCD predictions (86) and (87) completely in terms of the localized moments (82), which are insensitive to the behavior of the structure functions $f(x,Q^2)$ outside a given interval in x. We have thereby eliminated the model uncertainties in the comparison of these predictions with the experimental data. We shall use this circumstance and attempt to extract the QCD parameter Λ from the data. Its value will not contain uncontrolled systematic uncertainties associated with the arbitrariness in the choice of the x parametrization of the functions $f(x,Q^2)$.

To make the results more illustrative, we recall the widely accepted scheme for analyzing data on the basis of Eq. (80). First, it is necessary to establish the experimental values of the moments $\langle f_i\rangle_n$ for different Q_i^2. Since it is not the moments themselves that are measured but the functions $f(x,Q^2)$, the following method is used. We choose a certain parametrization

$$f(x,\ Q^2) = f(x,\ \{\alpha\}) \qquad (89)$$

with a set of free parameters $\{\alpha\}$. For each set of experimental points, obtained for $Q^2 = Q_i^2$, the corresponding set $\{\alpha_i\}$ is determined from the condition of best agreement between the parametrization (89) and these data. Then the analytic expressions (89) are integrated in accordance with (81), and the experimental values $\langle f_i^e\rangle_n$ of the moments are determined. The error $\Delta\langle f_i^e\rangle_n$ is expressed in terms of the uncertainties in the measurement of the function $f(x,Q_i^2)$ by means of the parameters $\{\alpha_i\}$. Knowing $\langle f_i^e\rangle_n$, we can turn to the verification of the relation (80). For this, we form the functional

$$\chi^2(\{\alpha_0\},\ \Lambda) = \sum_{i,n}\left(\frac{\langle f_i^e\rangle_n - \langle f^{\rm th}(\{\alpha_0\},\ s(Q_i^2,\Lambda))\rangle_n}{\Delta\langle f_i^e\rangle_n}\right)^2, \qquad (90)$$

where in accordance with (80)

$$\langle f^{\rm th}(\{\alpha_0\},\ s(Q_i^2,\ \Lambda))\rangle_n = \langle f(\{\alpha_0\})\rangle_n\, e^{\langle P\rangle_n s(Q_0^2,\Lambda)}. \qquad (91)$$

Unknown here are the parameters $\{\alpha_0\}$ of the initial conditions and the QCD parameter Λ. Their values are determined by minimizing χ^2. Such is the usual approach. A serious shortcoming of it is the model dependence of the procedure for finding $\langle f_i^e\rangle_n$, i.e., the dependence on the form of the parametrization (89). There is an uncertainty that seriously reduces the reliability of not only the extracted values of Λ but also the conclusions relating to the overall experimental status of QCD. The approaches in which Eqs. (78) for the functions $f(x,Q^2)$ rather than the relations for the moments are basic suffer from the same shortcoming. Below, this circumstance will be illustrated quantitatively.

We now turn to analysis of the data on the basis of the model-insensitive formulation of QCD in the form (86)–(87). The scheme of analysis is close to that described above. A difference is that in Eq. (90) it is necessary to replace the ordinary moments $\langle f\rangle_n$ by the localized ones $\langle f\rangle_n^{(k)}$:

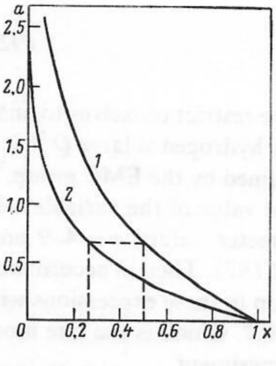

FIG. 13. Estimate of the effective interval of x from the maxima of the extreme terms: 1) $m = 2l$, $x_{\min} = e^{-2a}$; 2) $m = l$, $x_{\max} = e^{-a}$, $a = l/(n-1)$.

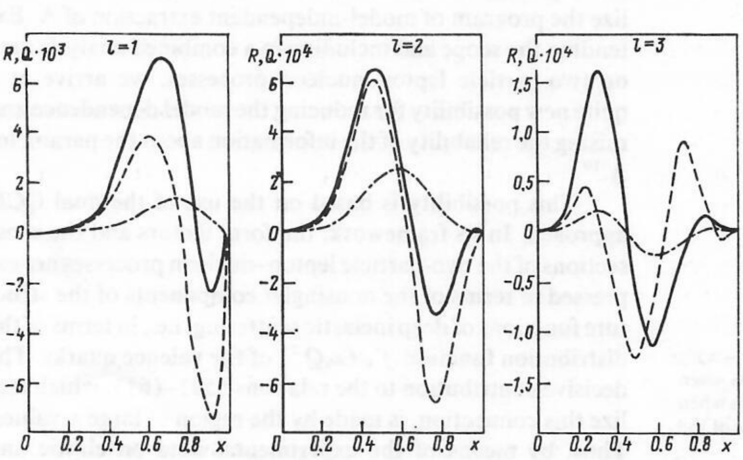

FIG. 14. Dependences of $R_n^l(x,s)$ and $Q_n^l(x,s)$ on x for $n = 8$. The continuous curve shows $R_n^l(x,0) = Q_l^n(x,0)$, the broken curve shows $R_n^l(n,s)$, and the chain curve shows $Q_n^l(x,s)$ for $s = 0.4$.

$$\langle f\rangle_n \to \langle f\rangle_n^{(2l)} - \sum_{k=l}^{2l-1} R_n^{l,k} \langle f\rangle_n^{(k)}. \tag{92}$$

To avoid further uncertainties, we restrict ourselves to analyzing data on muon scattering by hydrogen at large $Q^2(\gtrsim 2$ GeV$^2)$. Such data have been obtained by the EMC group.[76] In their experiment, the maximal value of the variable x is $x_{\max} = 0.65$. We take the parameter values $n = 4$–9 and $l = 3$ in the expressions (86) and (87). Then in accordance with Fig. 13 the main contribution to these expressions will be made by the region $0.2 \lesssim x \lesssim 0.7$, which is the one most saturated by data of the EMC experiment.

We shall find the moments $\langle f_i^e\rangle_n$ and $\langle f_i^e\rangle_n^{(k)}$ by using two types of parametrization—the very simple one $Ax^\alpha(1-x)^\beta$ and a more complicated one that follows from the model of Refs. 54 and 77. In addition, we shall fix the parameters $\{\alpha\}$ by using alternately data lying in the two ranges $x = 0.05$–0.65 and $x = 0.25$–0.65. Neither the one nor the other can produce a significant difference between the curves that model the function in the region $0.25 \leqslant x \leqslant 0.65$. There is here an appreciable number of experimental points with small errors, and this forces all the curves into a very narrow allowed corridor.

We have the opposite situation in the region $0.65 < x < 1$, in which there are no experimental points. Here, the modeling curves may differ arbitrarily strongly. Nevertheless, the use of the relations (96), in which this region is suppressed, must lead to a stable final result. But the relations (80) may given an appreciable spread in the parameter Λ. This is all reflected in Fig. 15, which gives the results of our analysis. We give the dependence $\chi^2(\Lambda)/\nu$ in all the variants listed above [$\nu = N_{\rm rel} - N_\alpha - 1$ is the number of degrees of freedom in the minimization of χ^2, $N_{\rm rel}$ is the number of relations employed in the sum (90), and N_α is the number of parameters $\{\alpha_0\}$ for Q_0^2].

It can be seen from Fig. 15 that the allowed values of the QCD parameter Λ lie in a very wide range. This means that the available experimental data on deep inelastic scattering enable us to extract almost no information about the parameter Λ without using model considerations. Numerical analysis shows[75] that to reduce the error in the determination of Λ to the level 30%–60% for a model-free determination the data must be made more accurate by almost an order of magnitude. If this could be achieved, we should have at our disposal information about the QCD parameter Λ "purified" of model uncertainties. As regards the values of this parameter that are now widely quoted in the literature with errors in the range 20%–50%, these results are essentially due to the choice of a particular x parametrization of the structure functions $f(x,Q^2)$. Such results can be given a certain correctness by using the predictions of physically motivated models in the choice of the x parametrization. For example, the statistical parton model with Regge asymptotic behavior[54,71] was used for this purpose in Refs. 55 and 71.

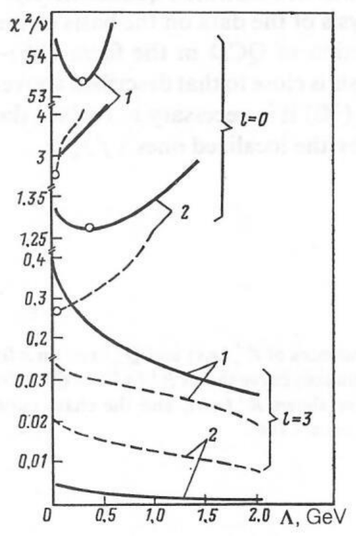

FIG. 15. Depedence of χ^2/ν on Λ: 1) the parametrization $Ax^\alpha(1-x)^\beta$; 2) in accordance with the model of Ref. 54. The continuous curve is when the range $x = 0.05$–0.65 is used to find $\{\alpha_i\}$, and the broken curve is when the range $x = 0.25$–0.65 is used. The open circles are the positions of the minima.

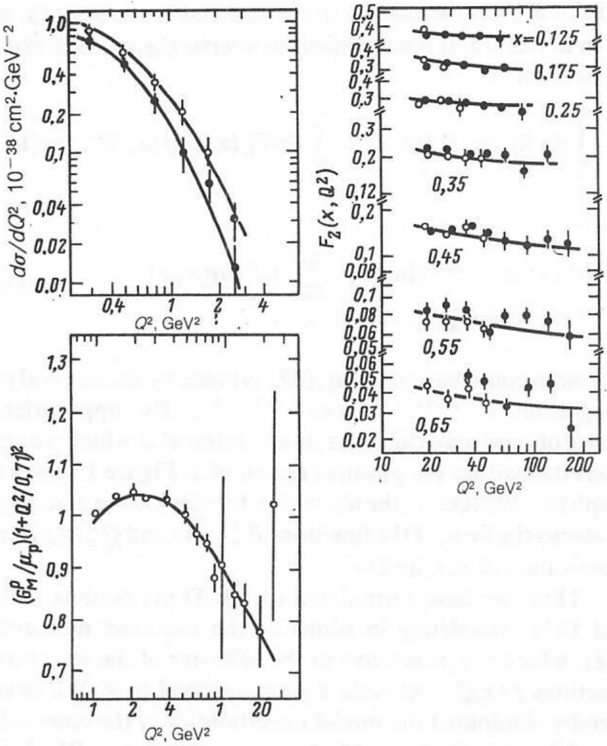

FIG. 16. Result of simultaneous analysis of data on the structure functions F_2 of deep inelastic scattering of muons by hydrogen,[76] the differential cross sections $d\sigma/dQ^2$ of the processes $\nu_\mu n \to \mu^- p$ (open circles) and $\bar\nu_\mu p \to \mu^+ n$ (black circles),[32] and the electromagnetic form factor G_M^p.[25]

Thus, if we remain in the framework of the existing data on deep inelastic lepton–nucleon scattering, we cannot realize the program of model-independent extraction of Λ. Extending the scope and including in a combined analysis data on two-particle lepton–nucleon processes, we arrive at a quite new possibility for reducing the model dependence and raising the reliability of the information about the parameter Λ.[19]

This possibility is based on the use of the dual QCD approach. In its framework, the form factors and the cross sections of the two-particle lepton–nucleon processes are expressed in terms of the nonsinglet components of the structure functions of deep inelastic scattering, i.e., in terms of the distribution function $f_V(x,Q^2)$ of the valence quarks. The decisive contribution to the relations (58)–(61), which realize this connection, is made by the region of large x values. Thus, by means of the experimental data on elastic and quasielastic lepton–nucleon processes one can catch the "tail" of the function $f_V(x,Q^2)$ in this region and thus reduce the main model uncertainties that derive from it. The most complete exploitation of this possibility consists of simultaneous analysis of the experimental data on the deep inelastic and two-particle lepton–nucleon processes.

In this analysis, the free parameters are the set of constants $\{\alpha\}$, which characterize the quark distribution at the normalization point Q_0^2, the QCD parameter Λ, and also the normalization constant Z and the mean transverse quark momentum p_T in the nucleon. We minimize the functional

$$\chi^2=\chi_0^2\ (\{\alpha\},\ \Lambda)+\sum_i\left[\frac{\left(\frac{d\sigma}{dQ^2}\right)^{e}-\frac{d\sigma}{dQ^2}\ (\{\alpha\},\ \Lambda,\ Z,\ p_T)}{\Delta\left(\frac{d\sigma}{dQ^2}\right)^{e}}\right]^2, \tag{93}$$

where χ_0^2 is determined by the expression (90), and $d\sigma/dQ^2$ are the cross sections of the elastic and quasielastic processes and are related to the form factors by Eq. (11). We analyze the experimental EMC data[76] on deep inelastic μp scattering, and also the data[25] on the proton electromagnetic form factors G_M^p and the cross sections $d\sigma/dQ^2$ of the $\nu n\to\mu^- p$, $\nu\bar{p}\to\mu^+ n$ processes.[32] The minimum of the functional (93) is attained for the following values of the free parameters:

$$p_T=(580^{+47}_{-53})\,\text{MeV};\ Z=3{,}29\pm0{,}07;\ \Lambda=(480^{+80}_{-100})\,\text{MeV}. \tag{94}$$

These numbers are almost independent of the choice of the x parametrization of the function $f_V(x,Q^2)$ in the class allowed by the χ^2 test, since its behavior is very severely restricted by the experimental data almost everywhere in the physical region of the variable $x\,(0.125\leqslant x\leqslant 1.0)$. The results of the analysis are given in Fig. 16. For our treatment, it is important to draw attention not so much to the absolute value $\Lambda=480$ MeV obtained for the parameter as to the error in its determination and the model independence. The absolute value of Λ is subject to a strong influence on the part of a number of factors that are difficult to take into account. For example, in the region of elastic and quasielastic data the threshold effects associated with successive activation of the quark flavors $s, c, \ldots$, etc., are very important.[78,79] There are also complexities that arise from the simultaneous analysis of the deep inelastic and two-particle processes. It would be desirable to eliminate from the treatment the singlet components of the structure functions. In the framework of the dual QCD approach they are not related to the nucleon form factors and, therefore, drop out of the scheme of the simultaneous analysis. From this point of view, the cleanest data are those on the structure function F_3 measured in νN scattering. Unfortunately, their accuracy is as yet insufficient for a restriction to be made to this set of data in the simultaneous analysis. All this has an uncontrollable effect on the extraction of the parameter Λ. Thus, absolute values of it must be treated very critically until the sources of the main uncertainties in the data analysis have been eliminated. We eliminate one of them—the model uncertainty.

The sharp decrease of the error in the determination of Λ when a simultaneous analysis of the data on the two-particle processes is included is noteworthy. We compare (94) with the results of independent analysis of the data on deep inelastic μp scattering: $\Lambda=(400^{+170}_{-150})$ MeV (see Fig. 15). The error has been reduced by almost two times, whereas the number of experimental points has been increased by only 40% by the inclusion of the two-particle processes. This is the main result of the simultaneous analysis, to which we wished to draw particular attention.

8. CONCLUSIONS

Thus, we have reviewed the present status of the theory and phenomenology of the two-particle lepton–nucleon processes at moderate momentum transfers Q^2. We have outlined the main tendencies in the development of theoretical ideas about the dynamics of these interactions based on QCD. We have demonstrated how fruitful it is to use dispersion sum rules. In this manner, we have succeeded in formulating satisfactory methods for calculating two-particle lepton–nucleon processes, and we have achieved good agreement with the experimental data. However, we must mention the semiphenomenological nature of the existing approaches to the description of these processes, this being necessitated by the allowance that must be made for the nonperturbative effects is in the region of intermediate energies.

In the review, we have presented two approaches based on the use of sum rules in QCD. One of them[14,15] is a development of the well-known method of QCD sum rules.[9] Its advantages are the wide cover of the phenomena of low-energy hadron physics and the sound physical basis. Thus, all the phenomenological parameters of the approach associated with the nonperturbative effects have a well-defined physical field-theoretical significance. This offers a prospect of well-founded hopes of rigorous calculation of them in the framework of QCD. Serious limitations on the applicability of this approach are imposed by the need to eliminate from the physical quantities a certain unphysical parameter always present in it. We may also mention a certain complexity of the applications of the approach to scattering problems. Therefore, only elastic electromagnetic eN scattering has so far been calculated in the framework of this approach.

The dual QCD approach developed by the authors of the review is much simpler in applications to all two-particle lepton–nucleon processes. It is fairly transparent, and calculations in its framework can be algorithmized. This has made it possible to calculate the electromagnetic and weak form factors of the nucleon, and also the cross sections of electroproduction and neutrino-induced production of the Δ_{33} isobar. The results of the dual QCD approach are in agreement with the available experimental data. Although this approach does not possess the generality inherent in the approach based on the QCD sum rules, it does enable one to establish a nontrivial connection between two-particle lepton–nucleon processes and deep inelastic processes. This is due to the fact that in the framework of the dual QCD approach the nucleon form factors are expressed in terms of the distribution functions of the valence quarks with respect to the fractions of the longitudinal nucleon momentum. These same functions occur in the expressions for the cross sections of deep inelastic scattering, and this made it possible to attack the problem of their simultaneous analysis with two-particle processes. An important result of such analysis is the more accurate determination of the fundamental QCD parameter Λ from the experimental data. It appears to us that already at the present time there exist approaches to the description of two-particle lepton–nucleon processes that are well founded in the framework of QCD. The use of their results for data analysis makes it possible to extract important physical information about nucleon structure. Especially topical in this connection, besides deep inelastic scattering, is a more detailed experimental study of exclusive processes.

We thank V. V. Ammosov, B. A. Arbuzov, S. A. Bunyatov, Yu. P. Ivanov, P. S. Isaev, A. V. Radyushkin, A. I. Mukhin, V. A. Petrov, and K. E. Shestermanov for helpful discussions and comments.

APPENDIX

The convolution kernels B_k are the Mellin transforms of the expansion parameters of the Wilson coefficient functions[72] and have the form

$$B_2(x)=\frac{4}{3}\,x\left\{2(1-x)\ln\frac{1-x}{x}+4x\left(\frac{\ln(1-x)}{1-x}\right)_+ -\left(\frac{2}{3}\pi^2+9\right)\delta(1-x)-\frac{3x}{(1-x)_+}-4x\frac{\ln x}{1-x}+4x+3\right\},$$

$$B_1(x)=B_2(x)-\frac{16}{3}x,\quad B_3(x)=B_2(x)-\frac{8}{3}x(1+x).$$

The generalized functions identified by the index $\langle\langle+\rangle\rangle$ are determined by the rules of integration

$$\int_0^1 dx\,\frac{h(x)}{(1-x)_+}=\int_0^1 dx\,\frac{h(x)-h(1)}{(1-x)};$$

$$\int_0^1 dx\,h(x)\left(\frac{\ln(1-x)}{1-x}\right)_+=\int_0^1 dx\,[h(x)-h(1)]\left(\frac{\ln(1-x)}{1-x}\right),$$

where $h(x)$ is a function that is regular at the boundary points. In practical calculations one must deal with integrals with a variable lower limit. From the definition of the generalized functions there follow the rules of integration

$$\int_a^1 dx\,\frac{h(x)}{(1-x)_+}=h(1)\ln(1-a)+\int_a^1 dx\,\frac{h(x)-h(1)}{(1-x)};$$

$$\int_a^1 dx\left(\frac{\ln(1-x)}{1-x}\right)_+=h(1)\,\frac{1}{2}\ln^2(1-a)+\int_a^1 dx\,(h(x)-h(1))\,\frac{\ln(1-x)}{1-x}.$$

The splitting function $P(x)$ has the form

$$P(x)=\frac{4}{3}\left[\frac{1+x^2}{(1-x)_+}+\frac{3}{2}\delta(1-x)\right].$$

[1]V.A. Matveev, R. M. Muradyan, and A. N. Tavkhelidze, Lett. Nuovo Cimento **7**, 719 (1973).
[2]S. J. Brodsky and G. R. Farrar, Phys. Rev. Lett. **31**, 1153 (1973).
[3]A. V. Radyushkin, Preprint R2-10717 [in Russian], JINR, Dubna (1977).
[4]S. J. Brodsky and C. P. Lepage, Preprint SLAC-Pub 2294.
[5]A. V. Efremov and A. V. Radyushkin, Phys. Lett. **94B**, 245 (1980).
[6]V. L. Chernyak, in: Materialy XV zimneĭ shkoly LIYaF (Proc. of the 15th Winter School of the Leningrad Institute of Nuclear Physics), Vol. 1 (1980), p. 65.
[7]F. M. Littes and A. V. Radyushkin, Yad. Fiz. **34**, 529 (1981) [Sov. J. Nucl. Phys. **34**, 293 (1981)].
[8]A. V. Radyushkin, Acta Phys. Pol. **B15**, 401 (1984).
[9]M. A. Shifman, A. I. Vainshtein, and V. I. Zakharov, Nucl. Phys. **B147**, 385 (1979).
[10]S. N. Nikolaev and A. V. Radyushkin, Nucl. Phys. **B213**, 285 (1983).
[11]M. B. Voloshin, Yad. Fiz. **29**, 1368 (1979) [Sov. J. Nucl. Phys. **29**, 703 (1979)].
[12]A. V. Smilga, Yad. Fiz. **35**, 473 (1982) [Sov. J. Nucl. Phys. **35**, 271 (1982)].
[13]L. J. Reinders, Acta Phys. Pol. **B15**, 329 (1984).
[14]V. A. Nesterenko and A. V. Radyushkin, Phys. Lett. **115B**, 410 (1982).
[15]B. L. Ioffe and A. V. Smilga, Phys. Lett. **114B**, 353 (1982); Nucl. Phys. **B216**, 373 (1983).
[16]S. G. Kovalenko, Soobshchenie (Communication) R2-80-499, JINR, Dubna (1980).
[17]A. A. Bel'kov, L. A. Klimenko, and S. G. Kovalenko, Preprint 83-30 [in Russian], Institute of High Energy Physics, Serpukhov (1983).
[18]A. A. Bel'kov, Yu. P. Ivanov, and S. G. Kovalenko, Yad. Fiz. **40**, 1301 (1984) [Sov. J. Nucl. Phys. **40**, 827 (1984)].
[19]A. A. Bel'kov, Yu. P. Ivanov, and S. G. Kovalenko, Preprint R2-84-348 [in Russian], JINR, Dubna (1984).
[20]M. Rosenbluth, Phys. Rev. **79**, 615 (1950).
[21]L. W. Mo and Y. S. Tsai, Rev. Mod. Phys. **41**, 205 (1969).
[22]J. Litt, G. Bushchhorn, D. H. Coward, *et al.*, Phys. Lett. **31B**, 40 (1970).
[23]L. E. Price, J. R. Dunning, M. Goitein, *et al.*, Phys. Rev. D **4**, 45 (1971).
[24]W. Bartel, F.-W. Büsser, W.-R. Dix, *et al.*, Nucl. Phys. **B58**, 429 (1973).
[25]P. N. Kirk, M. Breidenbach, J. I. Friedman, *et al.*, Phys. Rev. D **8**, 63 (1973).
[26]B. Bartoli, F. Felicetti, and V. Silvestrini, Rev. Nuovo Cimento **2**, 241 (1972).
[27]S. Stein, W. B. Atwood, and E. D. Bloom, Phys. Rev. D **12**, 1884 (1975).
[28]M. G. Olson, E. T. Osypovski, and E. H. Monsay, Phys. Rev. D **17**, 2938 (1978).
[29]N. J. Baker, A. M. Cnops, P. L. Connolly, *et al.*, Phys. Rev. D **23**, 2499 (1981).
[30]K. L. Miller, S. J. Barish, A. Engler, *et al.*, Phys. Rev. D **26**, 537 (1982).
[31]V. V. Makeev, A. G. Myagkov, A. Yu. Polyarush, *et al.*, Pis'ma Zh. Eksp. Teor. Fiz. **34**, 418 (1981) (JETP Lett. **34**, 397 (1981)].
[32]S. V. Belikov, A. P. Bugorskiĭ, A. A. Volkov, *et al.*, Yad. Fiz. **35**, 59 (1982) [Sov. J. Nucl. Phys. **35**, 35 (1982)].
[33]M. Pohl. L. Welch, M. Dewit, *et al.*, Phys. Lett. **72B**, 489 (1978).
[34]W. Lee, E. Madri, W. Sippach, *et al.*, Phys. Rev. Lett. **37**, 186 (1976).
[35]R. Entenberg, J. Horstkotte, W. Kozanecki, *et al.*, Phys. Rev. Lett. **42**, 1198 (1979).
[36]L. Segnal, in: Proc. of the European Physical Society Intern. Conf. on High Energy Physics, Geneva, 1979 (ed. A. Zichichi), CERN, Geneva (1980), p. 98.
[37]S. G. Kovalenko and A. V. Sidorov, Pis'ma Zh. Eksp. Teor. Fiz. **31**, 491 (1980) [JETP Lett. **31**, 461 (1980)].
[38]D. Le Yaouanc, L.Oliver, O. Pene, and J.-C. Raynal, Nucl. Phys. **B37**, 541 (1972).
[39]A. F. Pashkov, N. B. Skachkov, and I. K. Solovtsov, Pis'ma Zh. Eksp. Teor. Fiz. **25**, 452 (1977) [JETP Lett. **25**, 423 (1977)]; Communication R2-12003 [in Russian], JINR, Dubna (1979).
[40]V. G. Kadyshevsky, R. M. Mir-Kasimov, and N. B. Skachkov, Nuovo Cimento **55A**, 233 (1968).
[41]H. Harari and H. J. Lipkin, Phys. Rev. **140**, 1617 (1965).
[42]C. Becchi and G. Morpurgo, Phys. Lett. **17**, 352 (1965).
[43]M. Gourdin and P. Salin, Nuovo Cimento **27**, 193 (1963).
[44]D. J. Drickey and R. F. Mozley, Phys. Rev. Lett. **8**, 291 (1962).
[45]J. D. Bjorken and J. D. Walecka, Ann. Phys. (N. Y.) **38**, 35 (1966).
[46]W. Bartel, B. Dudelzak, H. Krehbiel, *et al.*, Phys. Lett. **28B**, 149 (1968).
[47]A. J. Dufner and Y. S. Tsai, Phys. Rev. **168**, 1801 (1969).
[48]S. J. Barish, M. Derrick, T. Dombeck, *et al.*, Phys. Rev. D **19**, 2521 (1979).
[49]P. Allen, J. Blietschau, H. Crässler, *et al.*, Nucl. Phys. **B176**, 269 (1980).
[50]N. J. Baker, A. M. Cnops, P. L. Connolly, *et al.*, Phys. Rev. D **23**, 2495 (1981).
[51]G. M. Radecky, V. E. Barners, D. D. Carmony, *et al.*, Phys. Rev. D **25**, 1161 (1982).
[52]S. Adler, Ann. Phys. (N. Y.) **50**, 189 (1968).
[53]P. Zucker, Phys. Rev. D **4**, 3350 (1971).
[54]P. S. Isaev and S. C. Kovalenko, Hadronic J. **3**, 919 (1980).
[55]V. A. Bednyakov, I. S. Zlatev, P. S. Isaev, and S. G. Kovalenko, Yad. Fiz. **36**, 745 (1982) [Sov. J. Nucl. Phys. **36**, 436 (1982)].
[56]V. A. Nesterenko and A. V. Radyushkin, Preprint E2-83-464 [in Eng-

lish], JINR, Dubna (1983); Yad. Fiz. **39**, 1287 (1984). [Sov. J. Nucl. Phys. **39**, 811 (1984)].
[57]B. L. Ioffe, Nucl. Phys. **B188**, 317 (1981).
[58]V. B. Belyaev and B. L. Ioffe, Zh. Eksp. Teor. Fiz. **83**, 876 (1982) [Sov. Phys. JETP **56**, 493 (1982)].
[59]S. Rock, SLAC-Pub-2449, Stanford (1982).
[60]E. D. Bloom and F. J. Gilman, Phys. Rev. D **4**, 2901 (1971).
[61]A. De Rújula, H. Georgi, and H. D. Politzer, Ann. Phys. (N. Y.) **103**, 315 (1977).
[62]A. De Rújula, H. Georgi, and H. D. Politzer, Phys. Rev. D **15**, 2495 (1977).
[63]R. K. Ellis, W. Furmanski, and R. Petronzio, Nucl. Phys. **B207**, 1 (1982).
[64]P. G. Freund, Phys. Rev. Lett. **20**, 1395 (1968).
[65]J. W. Moffat, Acta Phys. Austriaca Suppl. **9**, 605 (1972).
[66]R. P. Feynman, Photon–Hadron Interactions, Benjamin, Reading, Mass. (1972) [Russian translation published by Mir, Moscow (1975)].
[67]S. L. Glashow, J. Iliopoulos, and L. Maiani, Phys. Rev. D **2**, 1285 (1970).
[68]A. De Rújula, Phys. Rev. Lett. **32**, 1143 (1974).
[69]D. J. Gross and S. B. Treiman, Phys. Rev. Lett. **32**, 1145 (1974).
[70]V. V. Sudakov, Zh. Eksp. Teor. Fiz. **30**, 87 (1956) [Sov. Phys. JETP **3**, 65 (1956)].
[71]P. S. Isaev and Yu. P. Ivanov, Preprint E2-82-794 [in English], JINR, Dubna (1982).
[72]W. A. Bardin, A. J. Buras, D. W. Duke, and T. Muta, Phys. Rev. D **18**, 3998 (1978).
[73]L. N. Lipatov, Yad. Fiz. **20**, 181 (1974) [Sov. J. Nucl. Phys. **20**, 94 (1975)].
[74]G. Altarelli and G. Parisi, Nucl. Phys. **B126**, 298 (1977).
[75]Yu. P. Ivanov and S. G. Kovalenko, Yad. Fiz. **40**, 1277 (1984) [Sov. J. Nucl. Phys. **40**, 812 (1984)].
[76]J. J. Aubert, G. Bassompiere, K. H. Becks, *et al.*, Phys. Lett. **105B**, 315 (1981).
[77]V. A. Bednyakov, P. S. Isaev, and S. G. Kovalenko, Yad. Fiz. **40**, 1312 (1984) [Sov. J. Nucl. Phys. **40**, 834 (1984)].
[78]D. V. Shirkov, Yad. Fiz. **34**, 541 (1981) [Sov. J. Nucl. Phys. **34**, 300 (1981)].
[79]D. V. Shirkov, Teor. Mat. Fiz. **49**, 291 (1981).

Translated by Julian B. Barbour